AFATL-TR-88-85

Characterization of the Thermal Degradation of Selected Energetic Materials and Mixtures by Rapid-Scan Fourier Transform Infrared (RSFTIR) Spectroscopy

AD-A204 231

Thomas B Brill
Thomas P Russell

UNIVERSITY OF DELAWARE
DEPARTMENT OF CHEMISTRY AND BIOCHEMISTRY
NEWARK, DELAWARE 19716

SEPTEMBER 1988

INTERIM REPORT FOR PERIOD JUNE 1987 – JUNE 1988

AIR FORCE ARMAMENT LABORATORY
Air Force Systems Command ∎ United States Air Force ∎ Eglin Air Force Base, Florida

88 9 27 122

NOTICE

When Government drawings, specifications, or other data are used for any purpose other than in connection with a definitly Government-related procurement, the United States Government incurs no responsibility nor any obligation whatsoever. The fact that the Government may have formulated or in any way supplied the said drawings, specifications, or other data, is not to be regarded by implication, or otherwise as in any manner construed, as licensing the holder, or any other person or corporation; or conveying any rights or permission to manufacture, use, or sell any patented invention that may in any way be related thereto.

The AFATL STINFO Officer has reviewed this report, and it is releasable to the National Technical Information Service (NTIS), where it will be available to the general public, including foreign nationals.

This report has been reviewed and is approved for publication.

FOR THE COMMANDER
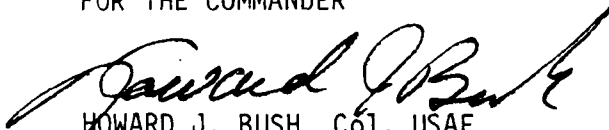
HOWARD J. BUSH, Col, USAF
Chief, Munitions Division

Please do not request copies of this report from the Air Force Armament Laboratory. Copies may be obtained from DTIC. Address your request for additional copies to:

Defense Technical Information Center
Cameron Station
Alexandria, VA 22304-6145

If your address has changed, if you wish to be removed from our mailing list, or if your organization no longer employs the addressee, please notify AFATL/MNE , Eglin AFB, FL 32542-5434, to help us maintain a current mailing list.

Copies of this report should not be returned unless return is required by security considerations, contractual obligations, or notice on a specific document.

REPORT DOCUMENTATION PAGE

Form Approved
OMB No. 0704-0188

1a. REPORT SECURITY CLASSIFICATION	1b. RESTRICTIVE MARKINGS
Unclassified	

2a. SECURITY CLASSIFICATION AUTHORITY	3. DISTRIBUTION/AVAILABILITY OF REPORT
	Approved for public release;
2b. DECLASSIFICATION/DOWNGRADING SCHEDULE	distribution is unlimited

4. PERFORMING ORGANIZATION REPORT NUMBER(S)	5. MONITORING ORGANIZATION REPORT NUMBER(S)
	AFATL-TR-88-85

6a. NAME OF PERFORMING ORGANIZATION	6b. OFFICE SYMBOL (If applicable)	7a. NAME OF MONITORING ORGANIZATION
University of Delaware		Energetic Materials Branch Munitions Division

6c. ADDRESS (City, State, and ZIP Code)	7b. ADDRESS (City, State, and ZIP Code)
Dept of Chemistry and Biochemistry Newark, DE 19716	Air Force Armament Laboratory Eglin AFB, FL 32542-5434

8a. NAME OF FUNDING/SPONSORING ORGANIZATION	8b. OFFICE SYMBOL (If applicable)	9. PROCUREMENT INSTRUMENT IDENTIFICATION NUMBER
Munitions Division	AFATL/MN	F08635-87-C-0130

8c. ADDRESS (City, State, and ZIP Code)	10. SOURCE OF FUNDING NUMBERS			
Air Force Armament Laboratory Eglin AFB, FL 32542-5434	PROGRAM ELEMENT NO.	PROJECT NO.	TASK NO	WORK UNIT ACCESSION NO.
	61102F	2303	E1	11

11. TITLE (Include Security Classification)
Characterization of the Thermal Degradation of Selected Energetic Materials and Mixtures by Rapid-Scan Fourier Transform Infrared (RSFTIR) Spectroscopy

12. PERSONAL AUTHOR(S)
Thomas B. Brill and Thomas P. Russell

13a. TYPE OF REPORT	13b. TIME COVERED	14. DATE OF REPORT (Year, Month, Day)	15. PAGE COUNT
Interim	FROM Jun 87 TO Jun 88	September 1988	53

16. SUPPLEMENTARY NOTATION
Availability of this report is specified on verso of front cover.

17. COSATI CODES			18. SUBJECT TERMS (Continue on reverse if necessary and identify by block number)
FIELD	GROUP	SUB-GROUP	Energetic Materials, Rapid-Scan Fourier Tranform
			Infrared Spectroscopy, Thermal Decomposition

19. ABSTRACT (Continue on reverse if necessary and identify by block number)

Infrared studies of the solid-melt phases of a homologous series of organobis (ammonium nitrate) salts (1,2-ethanediammonium dinitrate through 1,6-hexanediammonium dinitrate) are described. Fast thermolysis experiment involving selected organoammonium and organodiammonium nitrate salts are also described. Conclusions related to the solid phase and thermolysis studies are presented.

20. DISTRIBUTION/AVAILABILITY OF ABSTRACT	21. ABSTRACT SECURITY CLASSIFICATION
☐ UNCLASSIFIED/UNLIMITED ☒ SAME AS RPT. ☐ DTIC USERS	Unclassified

22a. NAME OF RESPONSIBLE INDIVIDUAL	22b. TELEPHONE (Include Area Code)	22c. OFFICE SYMBOL
Robert L. McKenney Jr.	(904) 882-3441	AFATL/MNE

DD Form 1473, JUN 86 — Previous editions are obsolete.

PREFACE

This program was conducted by personnel at the Department of Chemistry,
University of Delaware, Newark, DE 19716 under contract F08635-87-C-0130 with the
Air Force Armament Laboratory, Eglin AFB, FL 32542-5434. Dr. Robert L. McKenney,
Jr MNE managed the program for the Armament Laboratory. The program was conducted
during the period June 1, 1987 - May 31, 1988.

Accession For

NTIS GRA&I   ☒
DTIC TAB   ☐
Unannounced   ☐
Justification

By

Distribution/

Availability Codes

Dist | Avail and/or
     | Special

A-1

DTIC
COPY
INSPECTED
6

TABLE OF CONTENTS

LIST OF FIGURES

LIST OF FIGURES (CONCLUDED)

LIST OF TABLES

SECTION I

INTRODUCTION

The thermal decomposition of a homologous series of diammonium dinitrate salts is potentially interesting from a structure/property/ decomposition relationship point of view. The compounds 1,2-ethanediammonium dinitrate (EDD), 1,3-propanediammonuim dinitrate (PDD), 1,4-butanediammonium dinitrate (BDD) and 1,6-hexanediammonium dinitrate (HDD) were of interest.

Our particular direction has been to examine the Fourier transform infrared (FTIR) spectra of the solid and melt phases of these materials with the intention of exploring the ion motions that describe the condensed phase. A detailed study of the high heating rate thermolysis of BDD was then undertaken so that the decomposition characteristics of BDD at slow heating rates (5 - 60°C/min) could be compared to the behavior nearer the practical regime of ignition. To this end, rapid scan FTIR/Thermal profiling techniques employing heating rates up to 400°C/sec were used.

About one thousand separate thermolysis experiments have been performed in the course of this work. This Interim Report describes some of the representative results obtained for each system studied.

1

SECTION II

SOLID-MELT PHASE STUDIES OF EDD, PDD, BDD, and HDD

Work during this contract year has been directed inpart at the spectroscopic characterization of solid and melt phases of EDD, PDD, BDD, and HDD by transmission FTIR spectroscopy and differential scanning calorimetry (DSC). The combination of these two techniques permits identification of the first-order solid-solid and solid-liquid phase transitions. In some instances, the infrared (IR) spectral changes indicate the most likely structural changes that may be taking place.

1. IR STUDIES AT 23°C

It was observed that NaCl plates could not be used to study the IR spectrum of the dinitrate salts because the H_2O present facilitated ion exchange between the salt plate and the nitrate salt. Hence, spectra of $NaNO_3$ and the alkylammonium chloride salt contaminated the alkylammonium dinitrate spectrum. The phase transitions and melting points were also significantly affected. In fact, most of the anomalous spectral features could be mimiced by mixing various amounts of the alkylammonium nitrate and chloride salts and recording the spectra.

BaF_2 plates were successfully substituted for the NaCl plates in these studies. Thin films of EDD, PDD, BDD, and HDD were placed on a BaF_2 plate either by burnishing the sample into a transparent film with a spatula or by evaporating an ethanol/H_2O solution of the sample. The plate was then dried in vacuum for 48 hours. A second BaF_2 plate was placed over the sample and the two plates placed in a homebuilt cell designed for recording transmission IR spectra under slow heating conditions, Reference 1. The sample was heated at 3-4°C/min as measured by a thermocouple in contact with the sample. The temperature was verified by measuring the melting points of known standard compounds (±2°C). Spectra were recorded at 1 cm^{-1} resolution with 36 scans being added per file. The time to complete a spectral file is about 10 seconds. A Nicolet 60SX FTIR spectrometer with an MCT-B detector was used to record these spectra.

Figure 1 shows the IR spectra of EDD, PDD, BDD, and HDD recorded at 23°C on BaF_2 plates as described above. Table 1 gives the frequencies and suggested assignments for these mid-IR absorptions. These data are useful for reference

2

when examining the spectral changes as a function of temperature as described next.

2. IR AND DSC STUDIES ABOVE 23°C BUT BELOW THE DECOMPOSITION TEMPERATURE

a. EDD

By DSC (Figure 2), dry EDD in crimped pans heated at 5°C/min displayed phase transitions at 132°C, 145°C, and 172°C followed by melting (not shown) at 188°C. Additional uncertain effects seem to take place between 132-145°C. Figure 3 shows selected IR spectra as a function of temperature upon heating EDD from RT. These spectra were recorded on a sample obtained by grinding in EtOH with a few drops of H_2O. The solution was then evaporated on the BaF_2 plate in vacuum at RT for 48 hours. Because of the change in the transparency of the BaF_2 plate as a function of temperature, the background for each spectrum shown in this report was obtained with a BaF_2 plate heated to the same temperature.

$\nu_{as}(NO_3^-)$ centered at 1364 cm^{-1} shifts and changes intensity indicating that the motion of the ion is changing with temperature. The first phase transition becomes evident in the IR spectrum at about 134°C and is complete by about 140°C. The shape of $\nu_{as}(NO_3^-)$ and the C-C and C-N stretching modes (1040-1090 cm^{-1}) change markedly while the intensity of the $-NH_3^+$ deformation (1525 cm^{-1}) and the CH_2 scissors (1475 cm^{-1}) also change. This phase transition appears to involve some conformational change in the cation as evidenced by the significant change in the C-C and C-N stretching modes.

There is no spectral evidence in the mid-IR of the phase transition at 145°C indicating that the perturbation to the molecule is negligible. The phase transition at 172°C causes significant broadening of $\nu_{as}(NO_3^-)$ and the other modes except for $\nu(C-N)$ which narrows and becomes, more or less, a single absorption. The appearance of the spectrum of the solid phase above the 180°C, but below the melt, closely resembles that of the melt suggesting that this high temperature solid-solid phase transition is largely an order-disorder transition. The phase transitions are essentially reversible upon cooling.

b. PDD

By DSC (Figure 4) there is a solid-solid phase transition between 45 and 50°C. There is no evidence of this phase transition in the internal modes of the ions by IR spectroscopy (Figure 5). It must involve only a small

3

reorganization in the crystal lattice. These IR spectra were recorded in a sample dissolved in EtOH with a few drops of H_2O and then evaporated on a BaF_2 plate for 24 hours in vacuum. From RT to the melting point at 126°C, $\nu_{as}(NO_3^-)$ significantly and continuously changes indicating that increased anion motion is occurring as the temperature is raised. Melting is clearly evident at 126°C. The spectral changes are reversible.

 c. BDD

  By DSC no phase transitions occur in BDD from RT to the melting point at 140°C. Figure 6 shows the IR spectrum as a function of temperature. These were recorded on a sample that was dissolved in EtOH and allowed to evaporate in the BaF_2 plate under vacuum for 3 hours. Melting is detected at about 136°C, but is preceded by very substantial changes in the shape of $\nu_{as}(NO_3^-)$. Anion motion changes occur well in advance of the solid-liquid phase transition. Upon cooling this sample does not immediately return to the crystalline state suggesting that it remains amorphous for awhile. Similar behavior has been observed with other cigar-shaped molecules, Reference 2 and 3. We have not investigated the rate of crystallization of BDD from the melt, but it is definitely much slower to crystallize than EDD or PDD.

 d. HDD

  By DSC (Figure 7), HDD exhibits a multiple event phase transition at 65-72°C which preceded melting at 111°C. Figure 8 shows selected mid-IR spectra. The sample used for the IR work was dissolved in EtOH and placed on a BaF_2 plate. The solvent was removed by vacuum for several hours. The evidence for the solid-solid phase transition is largely confined to the CH_2 modes between $1400-1470 cm^{-1}$. $\nu_{as}(NO_3^-)$ gradually changes from RT up to the melting point. General line broadening and loss of resolution is evident at the melting point as a result of disorder of the ions in the lattice. HDD, like BDD, does not immediately crystallize, but remains amorphous on cooling.

SECTION III

## HIGH HEATING RATE THERMOLYSIS OF BDD

Experiments aimed at elucidating the decomposition mechanism of BDD at heating rates of 100-400°C/sec and static Ar pressures of 2-1000 psi were undertaken using the rapid-scan FTIR/temperature profiling technique, Reference 4. This technique is designed to follow in real time the gas products that appear several mm above the surface of the material while simultaneously measuring the temperature of the condensed phase. The temporal resolution of the FTIR spectra was 200 msec for these studies. That is, two complete mid-IR spectra were recorded every 100 msec and then every two consecutive files were combined to improve the spectral quality. The relative composition of the gas products was obtained by the use of the IR absolute intensities for each gas. Several observed products do not have known IR intensity values (HNCO, NH_4NO_3, and various amines). H_2O was not quantified because of the complicated rotation vibration fine structure.

In a second similar experiment, a fast-heat-and-hold study was performed using a somewhat modified homebuilt cell that permits ramp heating to a particular temperature and then holding that temperature while decomposition occurs, Reference 5.

1. FTIR/THERMAL PROFILING

In the 100-200°C/second heating rate range under 15 psi Ar, $HNO_3(g)$ is the first detected gas product. The temperature of its appearance varied between 200 and 320°C depending on the sample size and heating rate. However, the time of appearance clusters in the 280-300°C range. The melting temperature measured by DSC of about 140°C is close to the endotherm in the fast heating experiment. Figure 9 illustrates one set of data. The first evolved gas, HNO_3, is detected at about 280°C and is undoubtedly formed by the proton transfer reactions represented by Equations (1) and (2).

$$\left[\begin{array}{c} \bigcirc \end{array} \begin{array}{c} NH_3 \\ NH_3 \end{array} \right](NO_3)_2 \longrightarrow HNO_3(g) + \left[\begin{array}{c} \bigcirc \end{array} \begin{array}{c} NH_2 \\ NH_3 \end{array} \right]NO_3$$

(1)

5

$$\left[\text{(ring with NH}_3\text{ and NH}_3)\right](NO_3)_2 \longrightarrow 2\,HNO_3(g) + \text{(chain with NH}_2\text{ and NH}_2) \qquad (2)$$
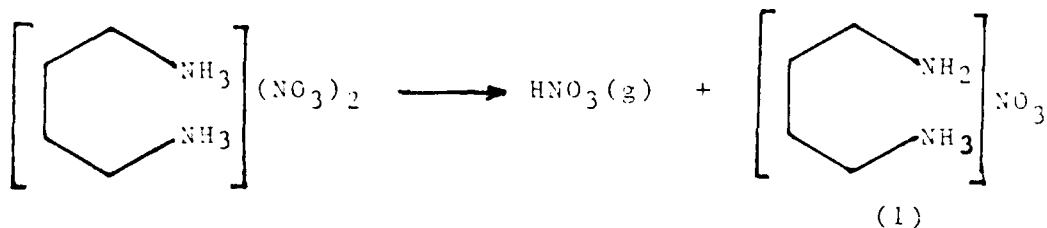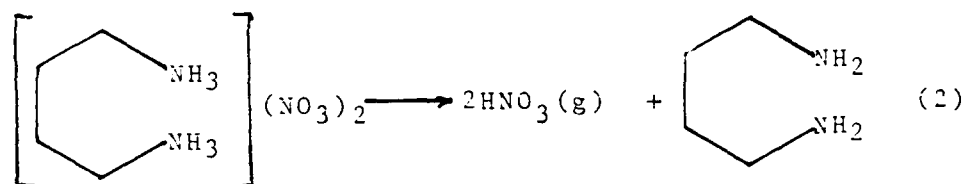
Within 0.2 - 0.4 seconds after the appearance of HNO_3, $NH_3(g)$ is detected. Then comes a gas which we recently determined to be pyrrolidine. The likelihood that this was the product was heightened by the coincidence of the absorptions at 2 cm^{-1} resolution with an authentic sample of pyrrolidine which was vaporized in the cell. Both NH_3 and pyrrolidine react with $HNO_3(g)$ to form NH_4NO_3 and pyrrolidinium nitrate as aerosols.

Plausible reaction sequences have been reported by McKenney and Struck, Reference 6, for the formation of these products.

$$\left[\text{(chain NH}_2\text{, NH}_3)\right]NO_3 \longrightarrow \left[\text{(ring NH}_2)\right]NO_3 + NH_3 \qquad (3)$$

$$\downarrow$$

$$\text{(ring) NH} + HNO_3 \qquad (3a)$$

$$\longrightarrow \left[\text{(ring NH}_3\text{, NH}_2)(NO_3)}\right] \longrightarrow \text{(ring) NH} + NH_4NO_3 \qquad (4)$$

$$\text{(chain NH}_2\text{, NH}_2) \longrightarrow \left[\text{(ring NH, NH}_3)}\right] \longrightarrow \text{(ring) NH} + NH_3 \qquad (5)$$

6
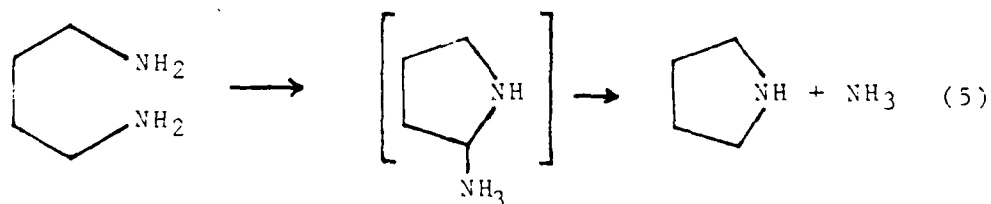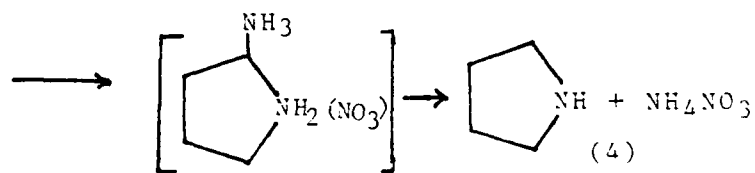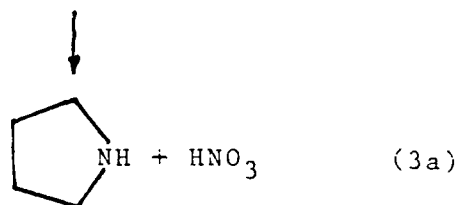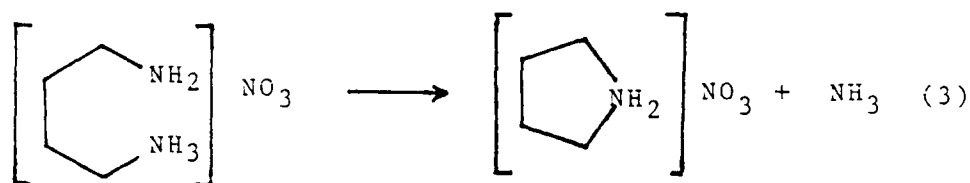
Because there is a smooth weight loss observed in the TGA, reactions represented by Equations (1) through (5) may all be occurring to liberate pyrrolidine, NH_3 and HNO_3. By using the present experiment, it is not possible to determine whether NH_3 is produced before, during or after the cyclization reaction. However, during all runs $NH_3(g)$ is detected before or at the same time pyrrolidine is detected leading to the possibility that reactions represented by Equations (3), (3a) and (5) may be favored. All of these reactions are consistent with Politzer's, Reference 7, theoretical findings that a $C-NH_3^+$ bond is weaker than a $C-NH_2$ bond and, therefore, is a favored point to form NH_3 by heterolysis.

As the sample continues to heat, $HNO_3(g)$ diminishes in concentration while $NO_2(g)$, $N_2O(g)$, $NO(g)$, and $CO_2(g)$ increase. $NH_3(g)$ stays relatively constant in concentration. CO_2 comes from backbone oxidation, but the nitrogen oxides are all known products of decomposition of HNO_3 and NH_4NO_3.

The time over which purely decomposition products are detected is decreased as the pressure is raised because the higher gas density reduces the diffusion rate of the gas products away from the samples, Reference 8. This effect is illustrated in Figure 10 with the thermolysis data at 40 psi Ar. $HNO_3(g)$ is still the initially detected gas product and forms at 295°C. This is followed by $NH_3(g)$ and pyrrolidine which then both react with the $HNO_3(g)$ to form NH_4NO_3 and pyrrolidinium nitrate. At about 305°C, an exotherm occurs that produces CO_2, C_2H_4, CO, C_2H_2, HCN, NO, $HNCO$, H_2O, and N_2O. In essence, the decomposition reactions have been driven farther along toward combustion-like products.

Under 100 psi Ar (Figure 11), $HNO_3(g)$ is no longer detected because the reaction zone is compressed. The decomposition reactions are driven farther toward the combustion regime. However, pyrrolidinium nitrate is still detected in the gas phase. The temperature at which the products appear remains at about 280°C and corresponds to a sharp exotherm. CH_4, CO_2, N_2O, C_2H_4, CO, HCN, NO, NH_3, H_2O, and $HNCO$ are the small molecule products.

The decomposition of BDD under 1000 psi Ar is similar to that at 100 psi with CO_2, CH_4, C_2H_4, HCN, CO, NO, NH_3, $HNCO$, and H_2O being the observed gas products. They appear at the exotherm at 275°C. Pyrrolidinium nitrate is still detected.

2. COMPARISON OF FAST-HEATING RATE DATA TO SLOWER HEATING-RATE DATA

It is of interest to compare the high-heating-rate thermolysis data for BDD to the slow-heating-rate data summarized in Table 2. By TGA the weight loss is a single-step process beginning at about 200°C and reaching 50 percent at about 260°C. The TGA experiment is, of course, a slow heating experiment (5°C/min) and, by nature, is not necessarily comparable to the fast heating data. Similarly, the DSC shows that the decomposition exotherm occurs in the 240-300°C range depending on the heating rate 5-60°C/min. Thus, TGA, DSC and the high-rate thermolysis data are all qualitatively consistent.

To improve the connection between the slow heating-rate (TGA/DSC) results and the high-rate data, the heating rate of the thermolysis cell was slowed to an intermediate heating rate range of about 25°C/sec (Figure 12). The melting endotherm occurs at about 130°C. $HNO_3(g)$ is detected at about 260°C and produces a slight endotherm as expected. About 2 seconds later $NH_3(g)$ is detected. AN(g) is detected along with several decomposition products (CO_2, N_2O, and NO) at about 300°C. At about 310°C, pyrrolidinium nitrate joins AN as a gas phase aerosol. A significant exotherm appears at about 320°C which corresponds to the disappearance of $HNO_3(g)$. The other products, NH_3, CO_2, N_2O, NO gas and AN and pyrrolidinium nitrate aerosol, remain. These data are consistent with those of the TGA in that the weight loss corresponds to many overlapped reactions and therefore shows no steps. The temperatures of the events are also consistent, in a general way, with the DSC data.

The above study indicates that $NH_3(g)$ is formed before the pyrrolidine appears which is most consistent with reactions represented by Equations (1), (3) and (3a) as the predominant decomposition sequence under these heating conditions.

3. FAST-HEAT-AND-HOLD STUDIES

Preliminary studies of BDD in which the sample was heated at a rate of about 200°C/sec were conducted. The final filament temperature (isothermal stage) was about 300°C, which is in the vicinity of the decomposition temperature of BDD. As shown in Figure 13, melting is detected in the expected range. At about 250°C some $HNO_3(g)$ and AN aerosol are observed. By 290°C pyrrolidinium nitrate joins AN as aerosols in the gas phase. The pyrrolidinium nitrate builds in concentration over the next several seconds at 300°C. These

8

data support the above conclusion that NH_3 is liberated before pyrrolidine in the thermolysis reaction. Another point of interest is that, qualitatively, AN(g) becomes higher in concentration relative to pyrrolidinium nitrate as the final thermolysis temperature is lowered. Since N_2O, NO, and H_2O are not prevalent at the lower thermolysis temperatures, this result probably originates from the fact AN(g) is not decomposed to these products and is able to build concentration.

FAST THERMOLYSIS OF PYRROLIDINIUM NITRATE

Because pyrrolidinium nitrate is detected in the gas phase, we were interested in knowing whether it could form in the condensed phase, then react to form neutrals, evaporate as neutrals, and reform as the salt aersol in the gas phase. To this end, an authentic sample of pyrrolidinium nitrate was prepared and its thermolysis studied. Figure 14 shows the thermal trace of a sample marked with the products detected. $HNO_3(g)$ is liberated essentially at room temperature and above which causes the sample thermal trace to lag far behind the reference thermal trace. Some unidentified gas products begin to appear at about 80°C. The compound exotherms at about 160°C. The IR spectrum of the first unidentified product matches closely to an authentic sample of N-nitroso-pyrrolidine which was evaporated in the cell. The reaction represented by Equation (6) has been postulated by McKenney and Struck, Reference 6, to explain the occurrence of this product in MS studies.

$$\left[\bigcirc NH_2 \right] NO_3 \xrightarrow{-H_2O} \bigcirc N-NO_2 \xrightarrow{+ \cdot H} \bigcirc N-NO + OH \cdot \quad (6)$$
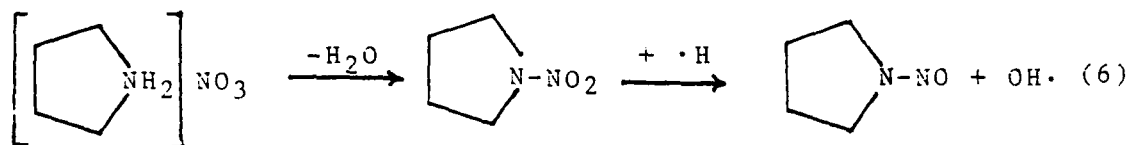
Further studies are anticipated on this reaction after obtaining an authentic sample of pyrrolidine nitramine and thermolyzing it.

The low temperature of decomposition of pyrrolidinium nitrate in the condensed phase suggests that it may not be formed as a salt in the condensed phase during the decomposition of BDD. This would be consistent with Equation (5). Since Equations (1), (3) and (3a) were also consistent with the data above on the decomposition reaction sequence of BDD, it would seem best to interpret the thermolysis of BDD to involve reactions represented by Equations (1) - (5) inclusive.

10

SECTION V

FAST THERMOLYSIS OF N-BUTYL MMC:''IM NITRATE

We were interested in comparing the thermolysis of the monoamine analog (BAN) of BDD to see how the results obtained for BDD might be related to other amines.

The IR-active gas products produced by 1-2mg of BAN at 130°C/second are shown in Figure 15. Superposed on these products is the reference and sample thermal trace. Initially a thermal lag occurs as a result of the greater thermal mass compared to the filament alone. An endotherm then occurs at 45°C which is close to the melting temperature obtained in other slow heating experiments. At 280°C the first gas product $HNO_3(g)$ is detected followed instantaneously by an unknown gas (Figure 16). By overlapping a gas phase spectrum of n-butylamine (Figure 17) and Figure 16, it can be seen that n-butylamine is a very good possibility for the unknown. At 310°C there is a second endotherm which corresponds to the evolution of $NH_3(g)$ possibly due to C-N bond fission and H migration occurring in the sample in the condensed phase. Also detected in this temperature region are CO_2 and N_2O gas possibly due to some backbone oxidation of the condensed phase or from the amine decomposing in the gas phase. $NO_2(g)$ is also detected early in the gas phase but is not quantified due to interfering peaks from the unknown. Approximately 0.5 seconds later the unknown gas product appears to become nitrated in the gas phase (Figure 18). By overlaying Figure 18 on the spectrum of solid phase n-butylammonium nitrate (Figure 19) it can be surmised that the unknown present initially with $HNO_3(g)$ is n-butylamine which has now been nitrated in the gas phase to form an aerosol of the starting material n-butylammonium nitrate. In Figure 18 and Figure 15 the $HNO_3(g)$ has been reduced to a negligible amount instantaneously upon the formation of the nitrate salt, while the $NH_3(g)$ is still present, but not quantifiable, due to the overlap of several peaks caused by the n-butylammonium nitrate in the gas phase.

From this work it can be seen that the proton transfer, desorption of the neutrals, and recombination in the gas phase takes place. The cyclization reaction appears to be peculiar to BDD even though NH_3 is liberated from BAN.

11

SECTION VI

FAST THERMOLYSIS OF PDD AND HDD

The thermolysis of PDD was investigated in the same spirit as was BAN with the intention of learning how nitrate salts closely related to BDD decompose relative to BDD.

In Figure 20 the reference and sample thermal trace is superposed on the IR-active gas products from 2-3 mg PDD under 15 psi Ar when heated at 140°C/sec. The difference trace is used here because of subtleties that are difficult to detect when the sample thermal trace alone is used.

The first endotherm occurs at 125°C corresponding to the melting temperature of PDD measured at slower heating rates (Table 2). The melt then continues to heat until 280°C where a second endotherm occurs and the first gas products are detected. $HNO_3(g)$ from proton transfer initially dominates, probably by a reaction analogous to that given above for BDD. $NH_3(g)$ is also detected in this temperature region. $NO_2(g)$ is found shortly after $HNO_3(g)$ is evolved. $NH_3(g)$ and $HNO_3(g)$ combine to generate $NH_4NO_3(g)$ which is detected, but not quantified. These events parallel those of BDD.

Above this temperature the behavior of PDD departs from that of BDD in that cyclization of the cation does not occur. Apparently the four-membered ring that would form is not sufficiently stable and the backbone breaks up. $C_2H_4(g)$ is detected from this step. The sample then continues to heat until 330°C where an exotherm occurs accompanied by the appearance of CO_2, N_2O, CO, NO, HCN, and NO_2 and the decrease in concentration $HNO_3(g)$. The products probably result from the oxidation of the backbone by $HNO_3(g)$. The exotherm under these conditions does not release enough heat to cause the sample temperature to exceed the reference thermal trace.

Figure 21 shows the IR-active gas products of PDD heated at 140°C/sec under 200 psi Ar. The superposed thermal profile of the sample is shown. Similarities exist between the results at this pressure and those shown in Figure 20. An endotherm is observed at 130°C. An exotherm resembling ignition occurs at 330°C which causes a sharp drop in the concentration of $HNO_3(g)$ and a sharp rise in the concentration of NO, CO, CO_2, HCN, H_2O, C_2H_4, C_2H_2, N_2O, and NO_2. This exotherm can be induced by as little as 40 psi Ar. The exotherm at all pressures above 15 psi causes the sample temperature to exceed the

12

reference filament temperature. The magnitude of the difference is accentuated as the pressure is increased.

In Figure 22 the IR-active gas products produced by rapid heating of HDD at 110°C/second under 15 psi Ar are shown. In this figure the thermal trace of the reference and sample are superposed on the IR-active gas products. The first endotherm at approximately 100°C corresponds to the melting temperature of HDD. The melt then heats to approximately 200°C/sec where $HNO_3(g)$ is detected due to proton transfer. Also, instantaneously after the appearance of $HNO_3(g)$, $NH_3(g)$ and an unknown gas are evolved simultaneously. We are intending to determine whether this unknown gas is α-ethylpyrrolidine. Almost instantly after its appearance, the unknown gas appears to be nitrated causing a sharp decrease in $HNO_3(g)$. Also the $NH_3(g)$ does not appear to be affected and stays relatively constant in relative percentage during the duration of the experiment. At 285°C an exotherm occurs coincident with the appearance of CO_2, NO, and N_2O. The remainder of the $HNO_3(g)$ decreases rapidly at this point probably due to its reduction to N_2O and NO.

Figure 23 shows the IR-active gas products of HDD at 110°C/second and under 100 psi Ar. The superposed thermal profile of the sample is shown. Similarities exist between the results at this pressure and those shown in Figure 21. An endotherm is observed at 100°C corresponding to the melting temperature of HDD. The melt heats to 240°C where exothermic ignition occurs releasing the IR-active products CO_2, N_2O, NO, CO, NH_3, C_2H_4, and HCN which are all quantified. HNCO and some unknown as described above are also released at the exotherm but are not qualified. Similar to the behavior 15 psi Ar, the unknown gas appears to become nitrated almost instantaneously after being evolved.

The decomposition of HDD resembles that of BDD in that proton transfer, C-N bond heterolysis and (possibly) cyclization takes place.

SECTION VII

AN/BDD MIXTURE STUDIES

The evidence for an endotherm near 400°C during the fast thermolysis of BDD (see Figure 9) has not yet been explained. We considered the possibility that it might originate from subliming NH_4NO_3, because of the endotherm for pure AN at 320°C (Figure 24). Heterogeneous mixtures of BDD and AN were prepared to test this possibility. Figure 25 shows the thermal trace of a 25/75 by weight mixture of AN/BDD. It can be seen that the melting endotherm at about 130°C is dominated by the BDD without much of a melting point depression. The AN sublimation endotherm in the 320°C range remains and is not altered by the presence of BDD. Hence, it appears that the condensed phase thermochemistry of these two compounds is roughly additive. The endotherm in BDD above 400°C is not brought on by the formation of AN.

SECTION VIII

CONCLUSIONS

1. SOLID PHASE

a. The NO_3^- ion displays a significant increase in motion (disorder) in the solid state as the temperature is raised. At the melting point, the NO_3^- ion is probably best described as a restricted rotor. Except possibly for EDD, the conformations of the cations do not appear to change during the solid-solid phase transitions.

b. After melting and cooling, BDD and HDD are best described as largely disordered solids. These two salts differ from EDD and PDD in this behavior.

c. As a caveat for similar future studies, the IR spectrum of solid samples of these nitrate salts is potentially complicated by ion exchange with similar sized anions in the support.

2. THERMOLYSIS STUDIES

a. The decomposition temperatures of the salts investigated here at fast heating rates resemble those measured by DSC/TGA at slow heating rates. The range of heating rates studied in this work differs by a factor of 2500. The temperature that the first detected decomposition products appear is hardly affected at all by applied pressure differences in the range of 15-1000 psi Ar.

b. HNO_3 is the first detected gas product in all cases.

c. NH_3 is the second detected gas product and appears before pyrrolidine in the thermolysis of BDD.

d. Both NH_3 and pyrrolidine react with HNO_3 in the gas phase to form nitrate salts as aerosols.

e. AN(g) is in higher concentration relative to pyrrolidinium nitrate when the final filament temperature is lower because the AN does not decompose to such a great extent to N_2O and H_2O at the lower temperatures.

f. Pyrrolidinium nitrate will not be present in the condensed phase at the decomposition temperature of BDD because it decomposes at and above room temperature and exotherms at 160°C. These temperatures are well below the decomposition temperature of BDD (275-300°C).

g. Arguments can be put forth that a complex series of early reactions is needed to describe the thermolysis of BDD. These include reactions represented

by Equations (1) through (5) that are described in the text. These explain all of the observations.

h. Thermolysis of BAN and PDD show the same early reactions as BDD but the cyclization step is absent.

i. HDD shows the same early reactions as BDD and a cyclization step occurs that will be investigated in the near future.

TABLE 1: INFRARED FREQUENCIES OF DINITRATE SALTS

EDD043	PDD042	EDD041	HDD040	TENTATIVE ASIGNMENTS
3217	3228	3217	3221	NH ASYM. + SYM. STRETCHING
3170	3150	3131	3193	
3123	3095	3068	3166	
			3095	
3052	2962	3017	3001	CH2 ASYM. +SYM. STRETCHING
2986	2915	2954	2978	
2825	2829	2884	2933	
		2810	2868	
**	**	**	**	
1605	1609	1629	1622	NH3+ASYM. DEF
		1594		
1527	1512	1519	1536	NH3+ SYM. DEF
		1491		
1476	1478	1477	1477	CH2 SCISSORS
		1453	1460	
	1418			
1364	1396	1360	1368	NO3- ASYM STR
	1358		1331	
	1324	1319	1307	NO3- ASYM STR
		1277		
	1220		1246	
	1197	1174		
		1142		
	1114	1104	1117	
1089				
		1058		
1041	1046	1042	1040	C-N STRETCHING
		1024		
	963		984	
	943	905	947	
		884		
		866		
824	823	822	824	NO3- BENDING
804				
784		787		NH3+ ROCKING
765	762	754		CH2 ROCKING

** All bands present between 2700cm-1 and 1600cm-1 are overtones and combinations.

TABLE 2. DSC AND TGA DATA FOR PHASE TRANSITIONS, MELTING, AND DECOMPOSITION

	EDD	PDD	BDD	HDD
TGA				
Tonset, °C	200	225	200	
$T_{50\%}$, °C	295	295-315	260	
DSC				
1st Order Phase Transition, °C	132	55	--	65, 73
Melting, °C	188	125	138(60)	108
Decomposition [a]	290(60)	310(60)	295(60)	265(60)
	275(20)	295(40)	290(40)	248(20)
	265(5)	295(20)	295(30)	
		260(5)	280(20)	
			240(10)	
			260(5)	

[a] parenthetical number is dT/dt in °C/min
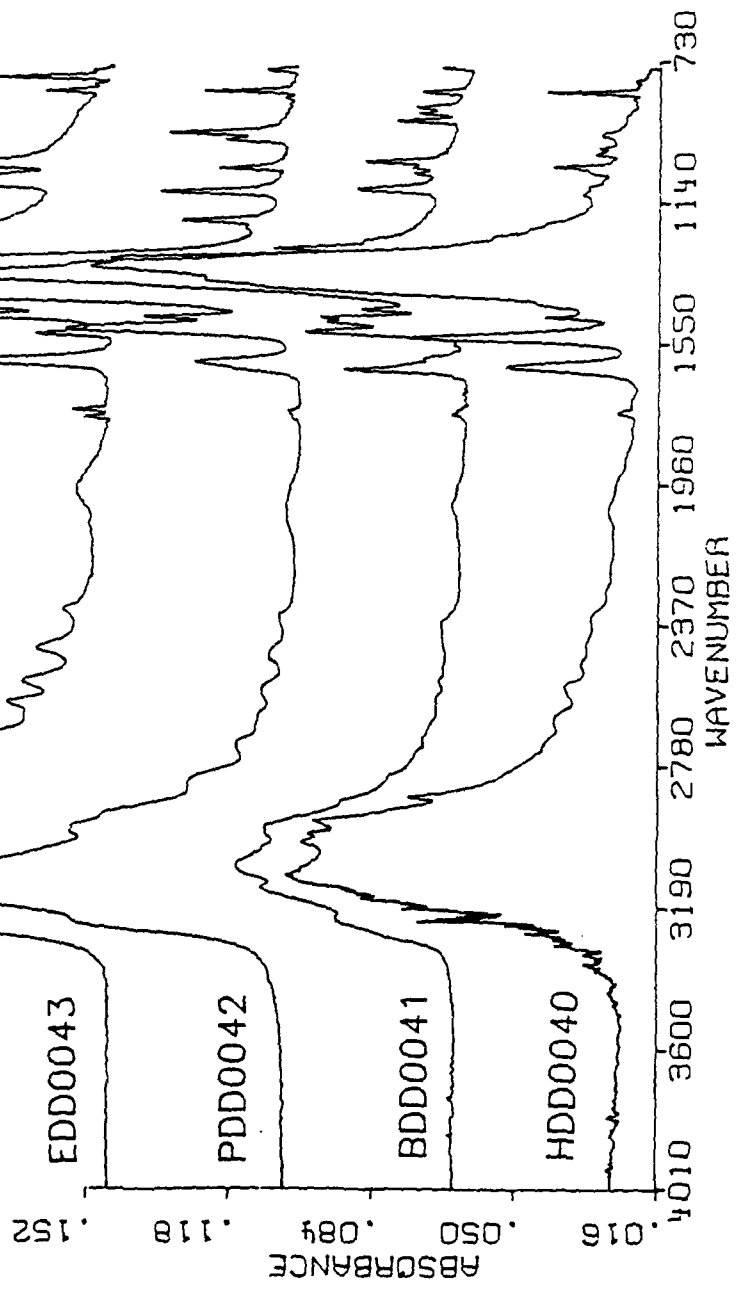
Figure 1. Transmission IR Spectra of Compounds at 23°C.

19

DSC

Sample: EDDN 5/MIN
Size: 2.3700 mg
Method: TPR
Comment: 5/DEG/MIN

File: DSCEDDN1.01
Operator: TPR
Run Date: 10/29/87   10:42
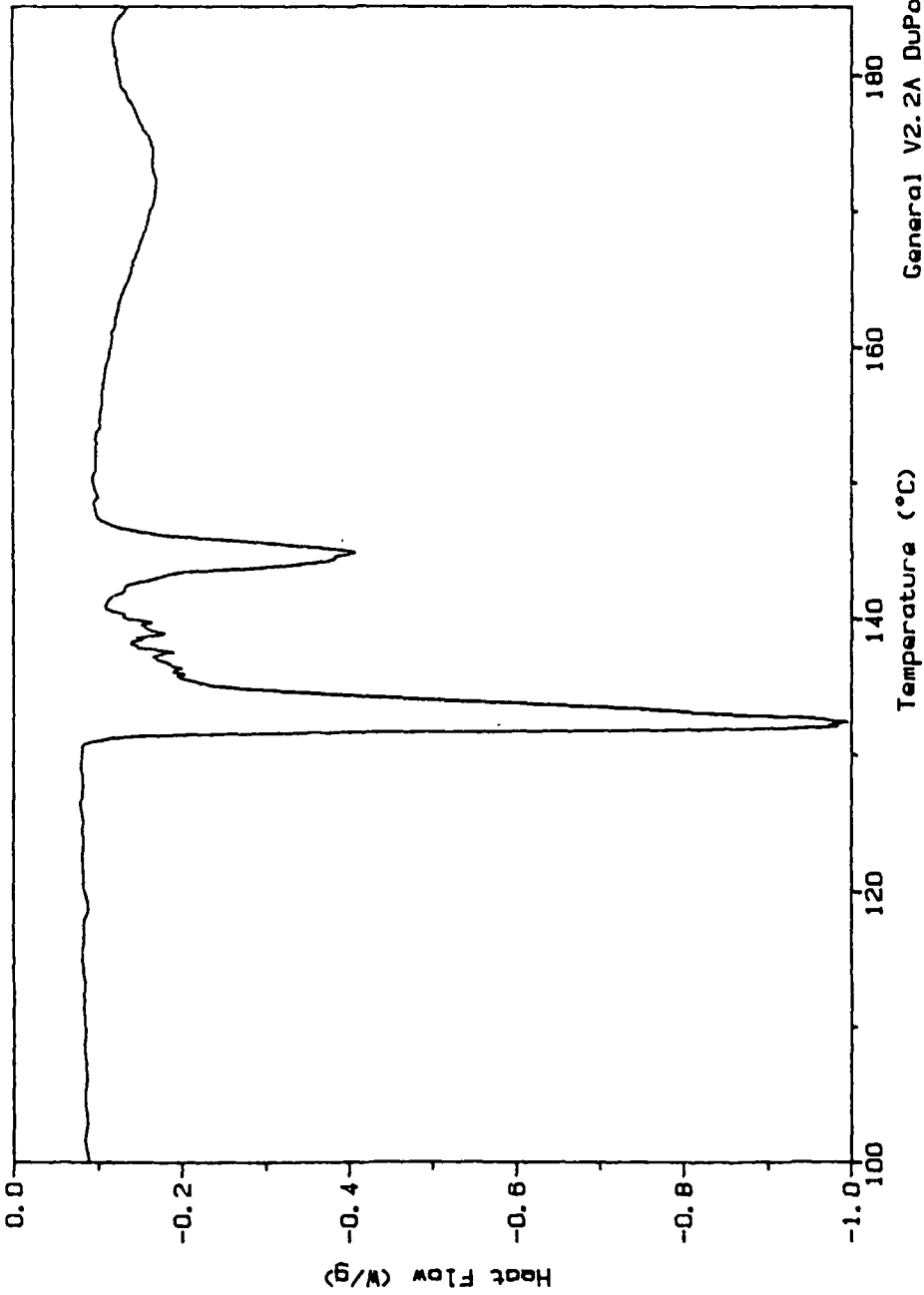
Figure 2.   DSC of EDD

General V2.2A DuPont 9900

20
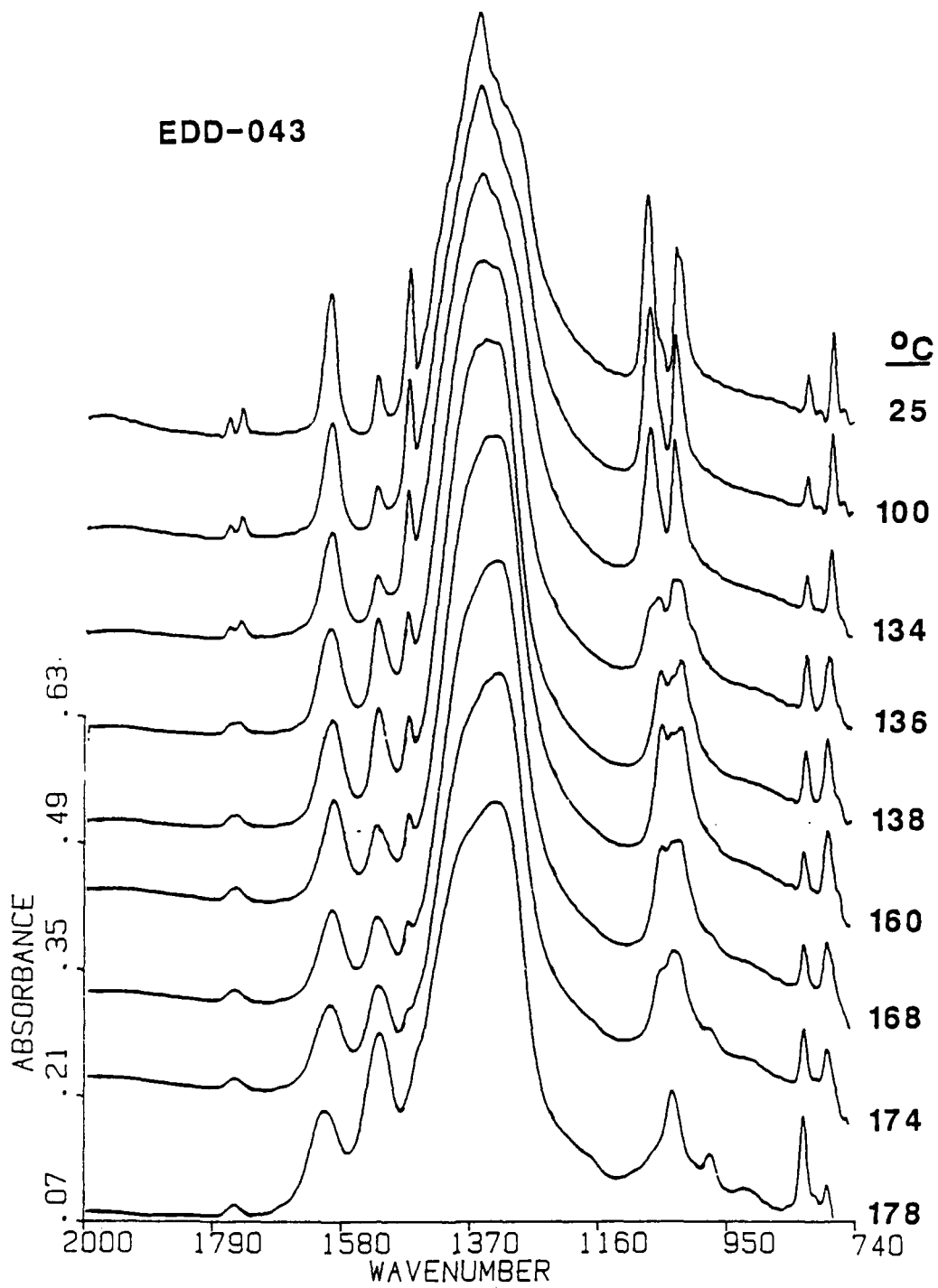
Figure 3.   Selected Transmission IR Spectra of EDD as a Function of Temperature

21
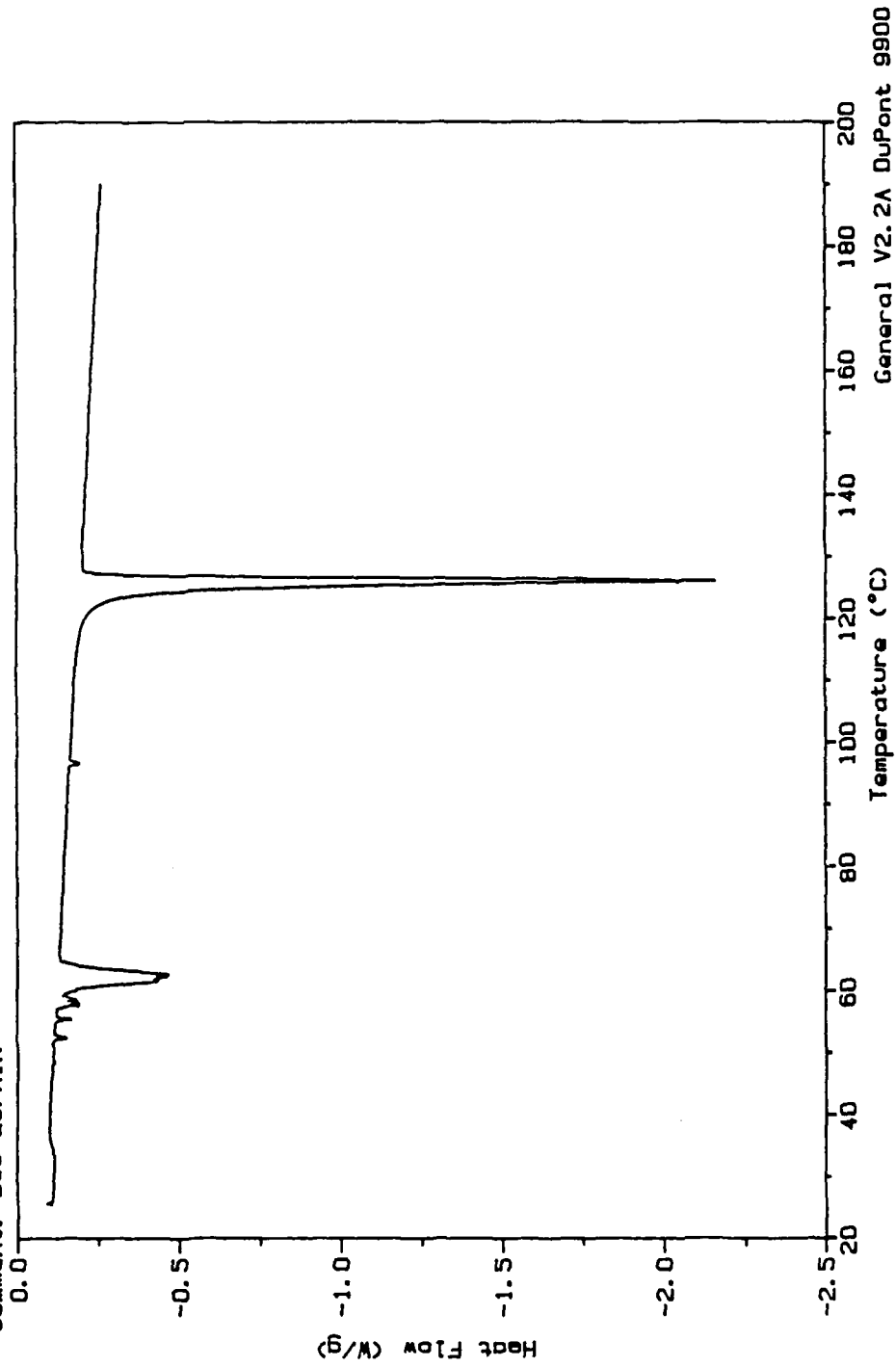
Figure 4. DSC of PDD
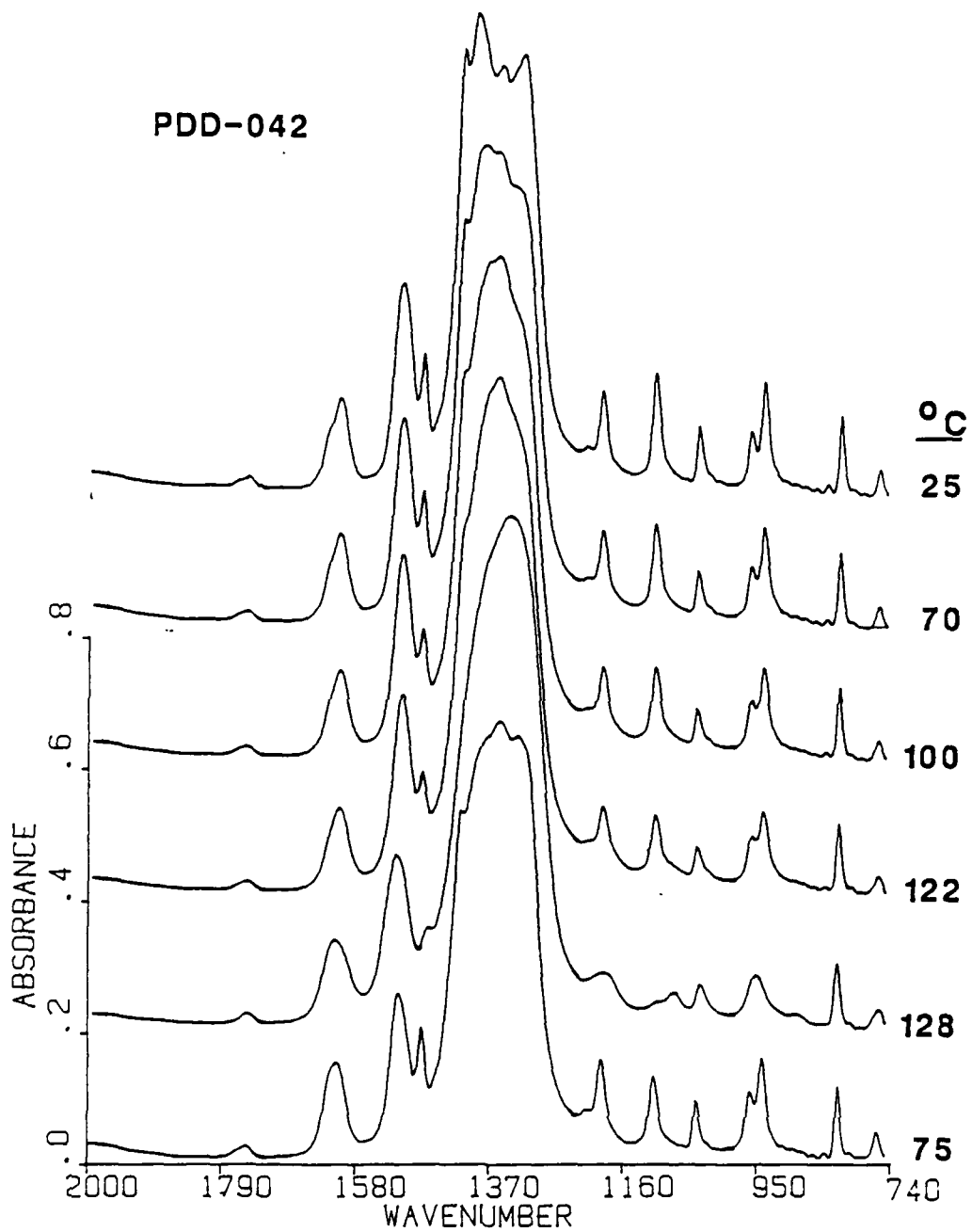
Figure 5.   Selected Transmission IR Spectra of PDD as a Function of Temperature
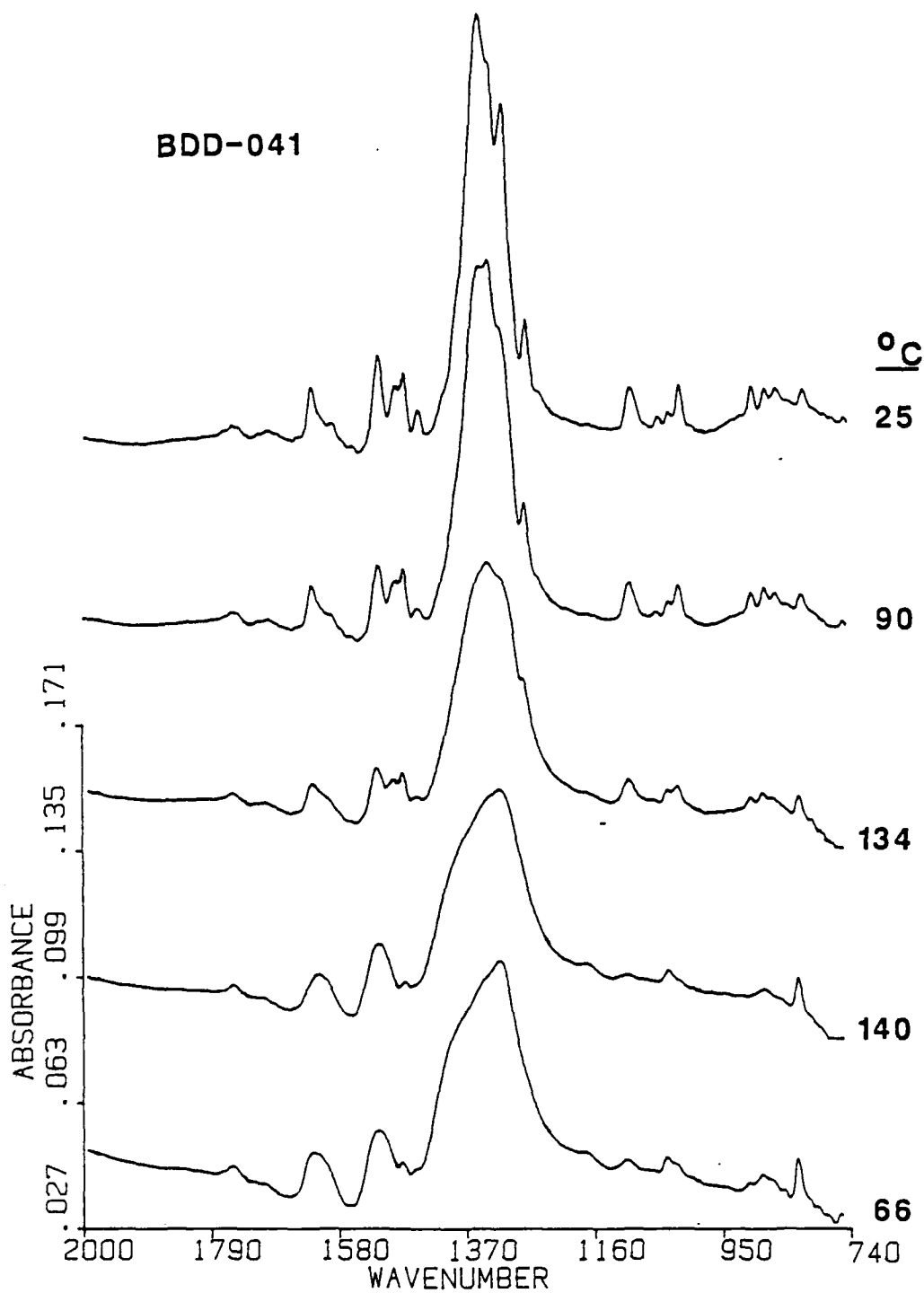
Figure 6. Selected Transmission IR Spectra of BDD as a Function of Temperature

24

Figure 7. DSC of HDD

25
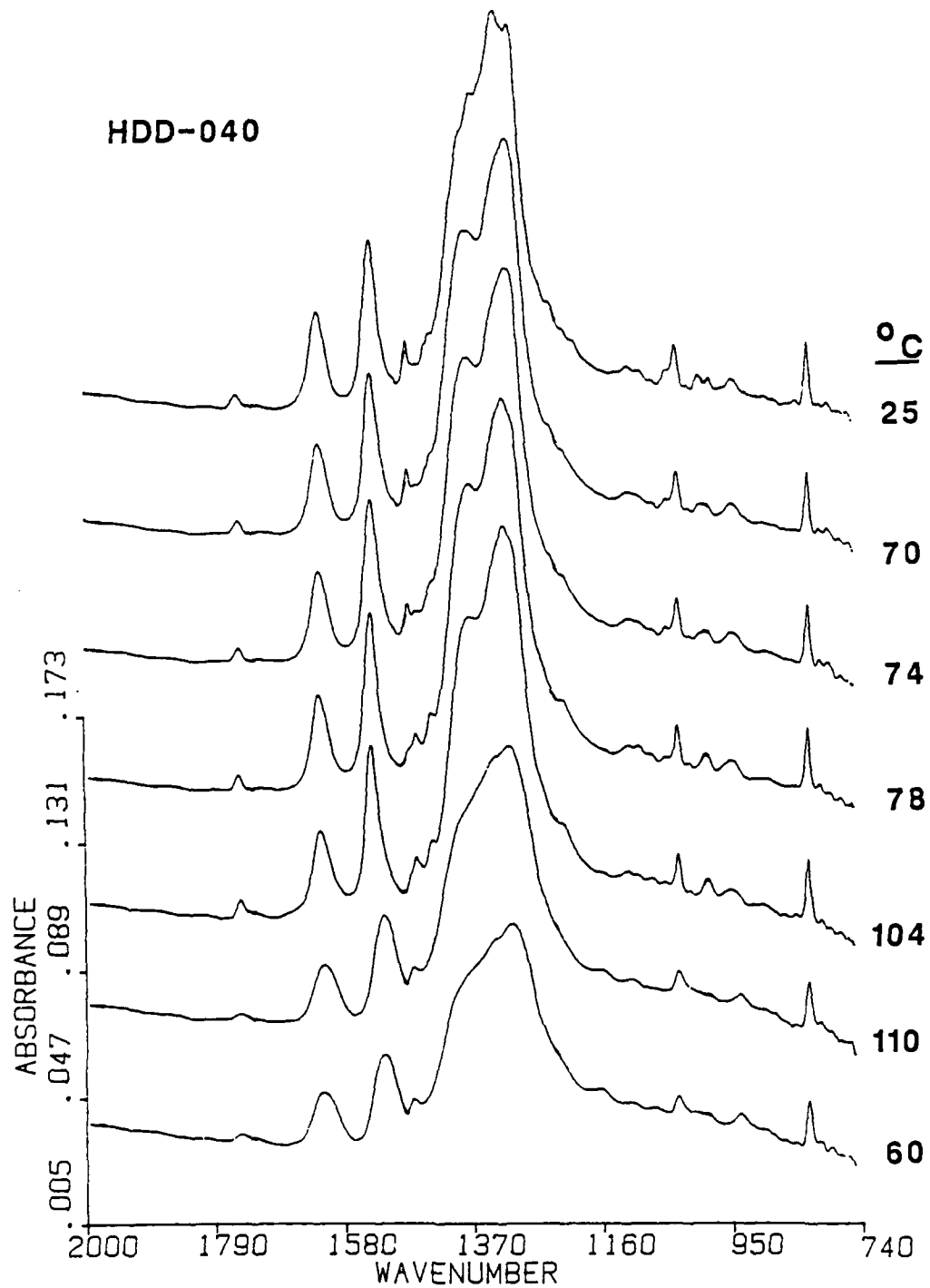
Figure 8. Selected Transmission IR Spectra of HDD as a Function of Temperature

26
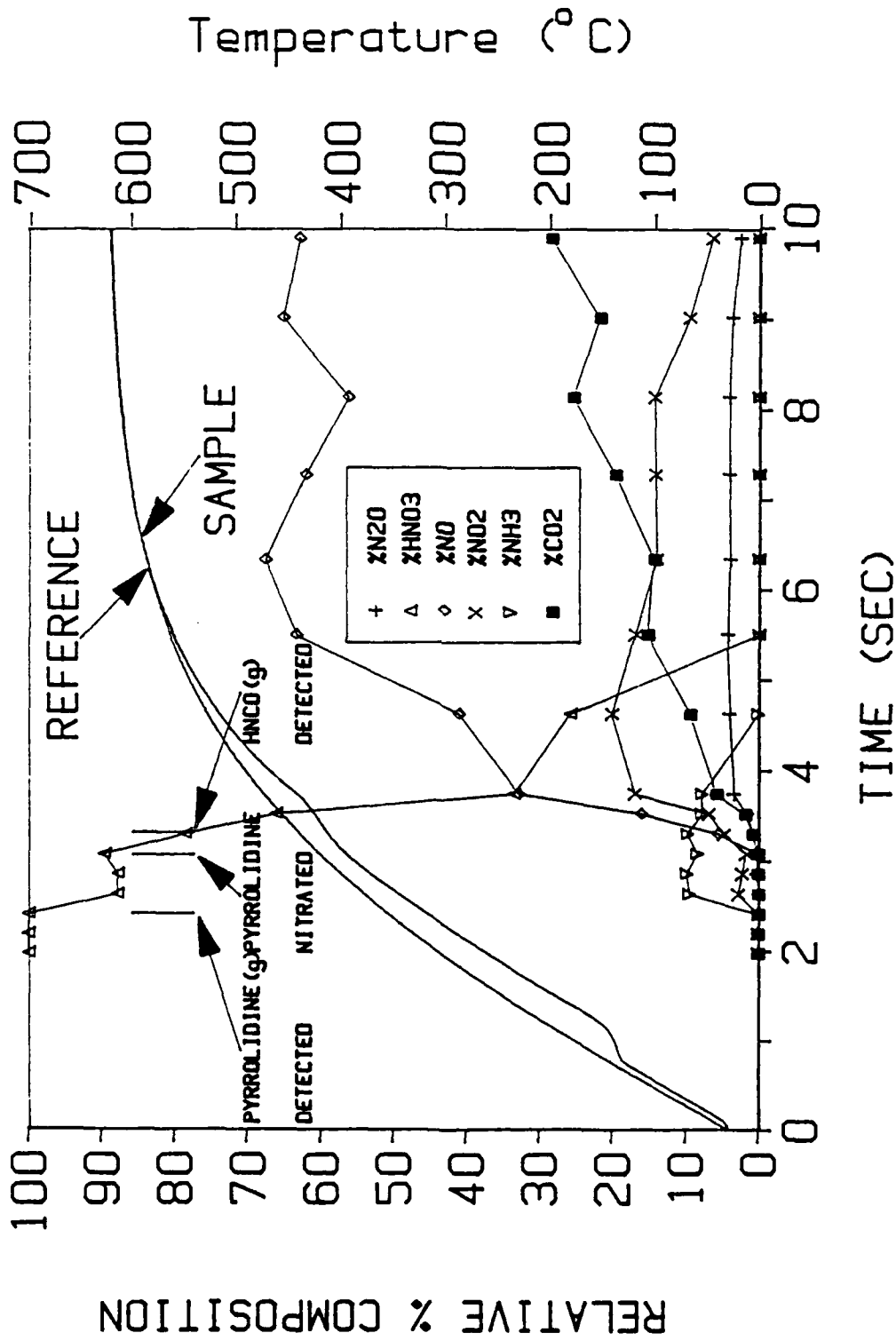
Figure 9.   The Relative Percent Concentration Versus Time Profile for BDD
Heated at 150°C/sec Under 15 psi Ar Superposed on the Thermal
Trace of the Condensed Phase.
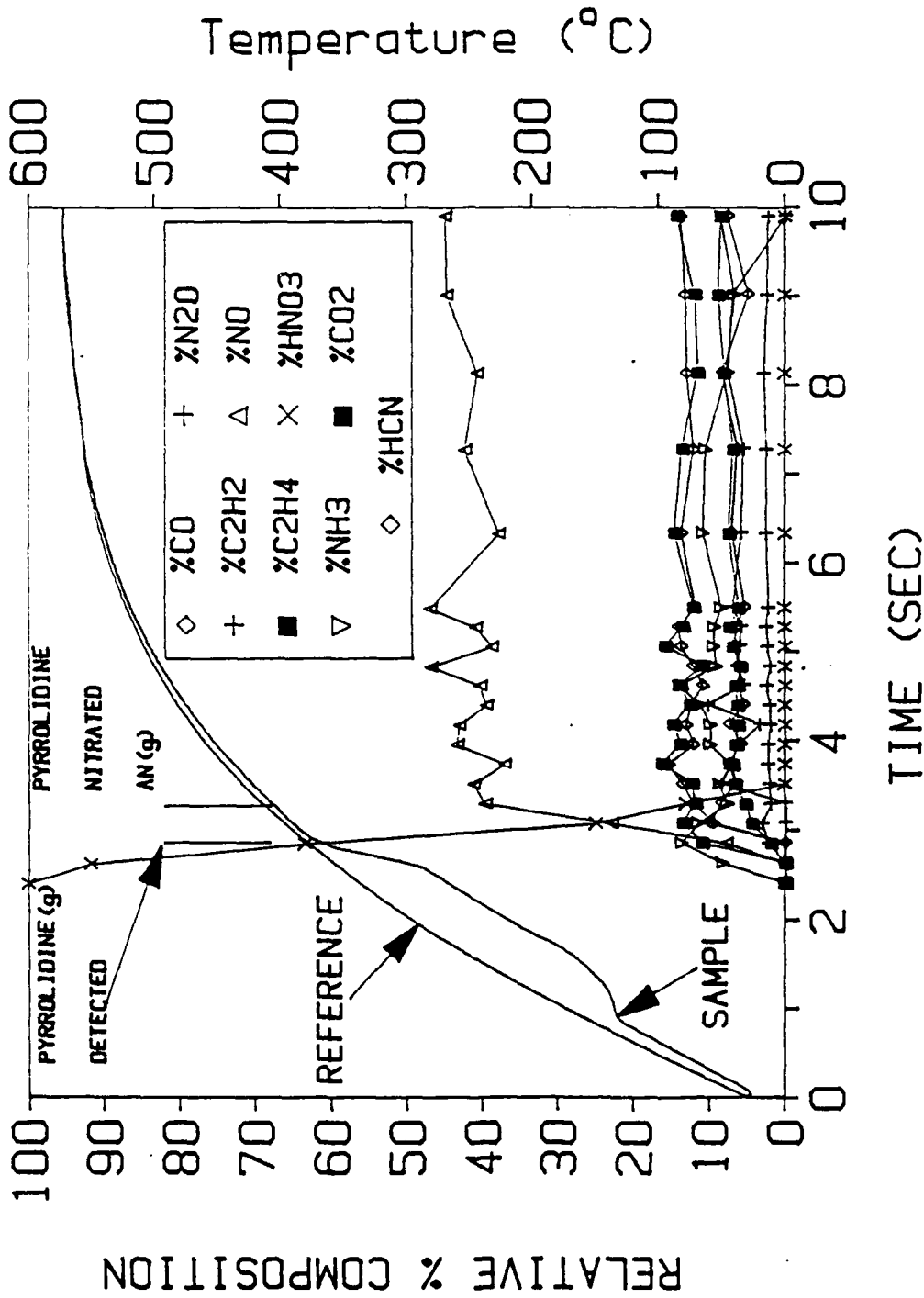
Figure 10. Relative Percent Concentration Versus Time Profile for B00 Heated at 100°C/sec Under 40 psi Argon Superposed on the Thermal Trace
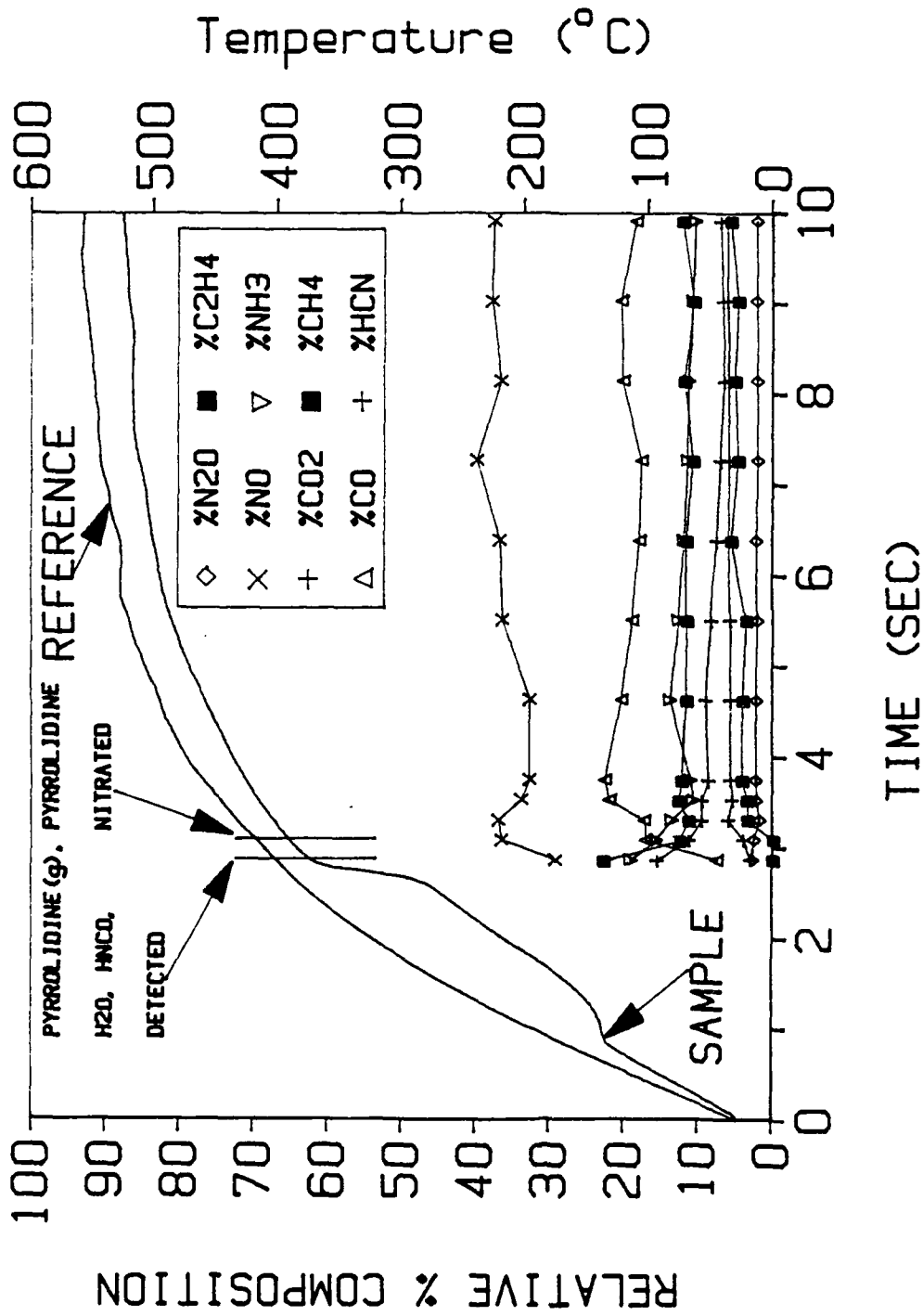
Figure 11. Relative Percent Composition Versus Time Profile for BDD Heated at 100°C/sec Under 100 psi Argon Superposed on the Thermal Trace

29
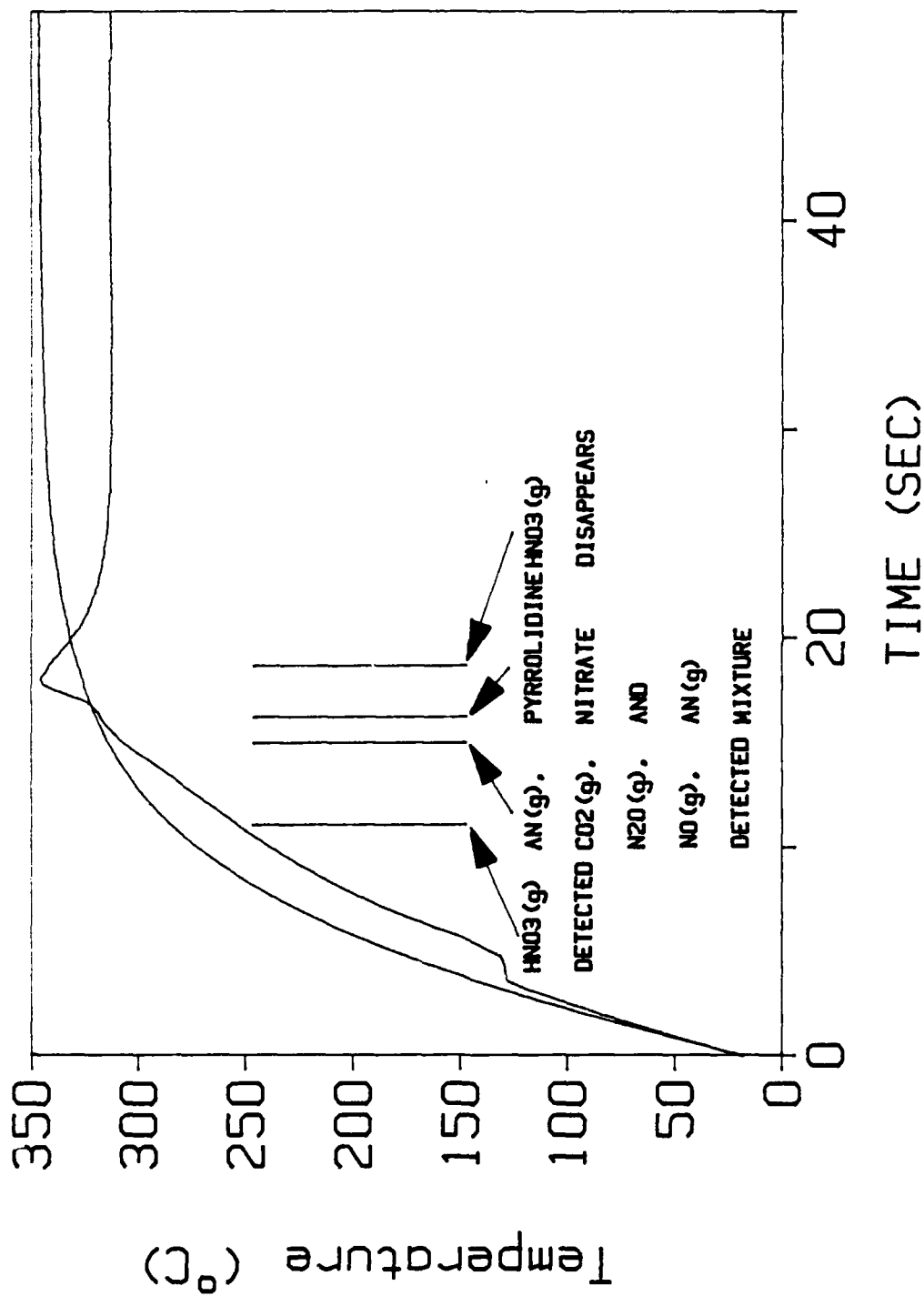
Figure 12.   Thermal Trace of the Condensed Phase of BDD Heated at
25°C/sec Showing the Time of Appearance of the Important Gas
Products

30
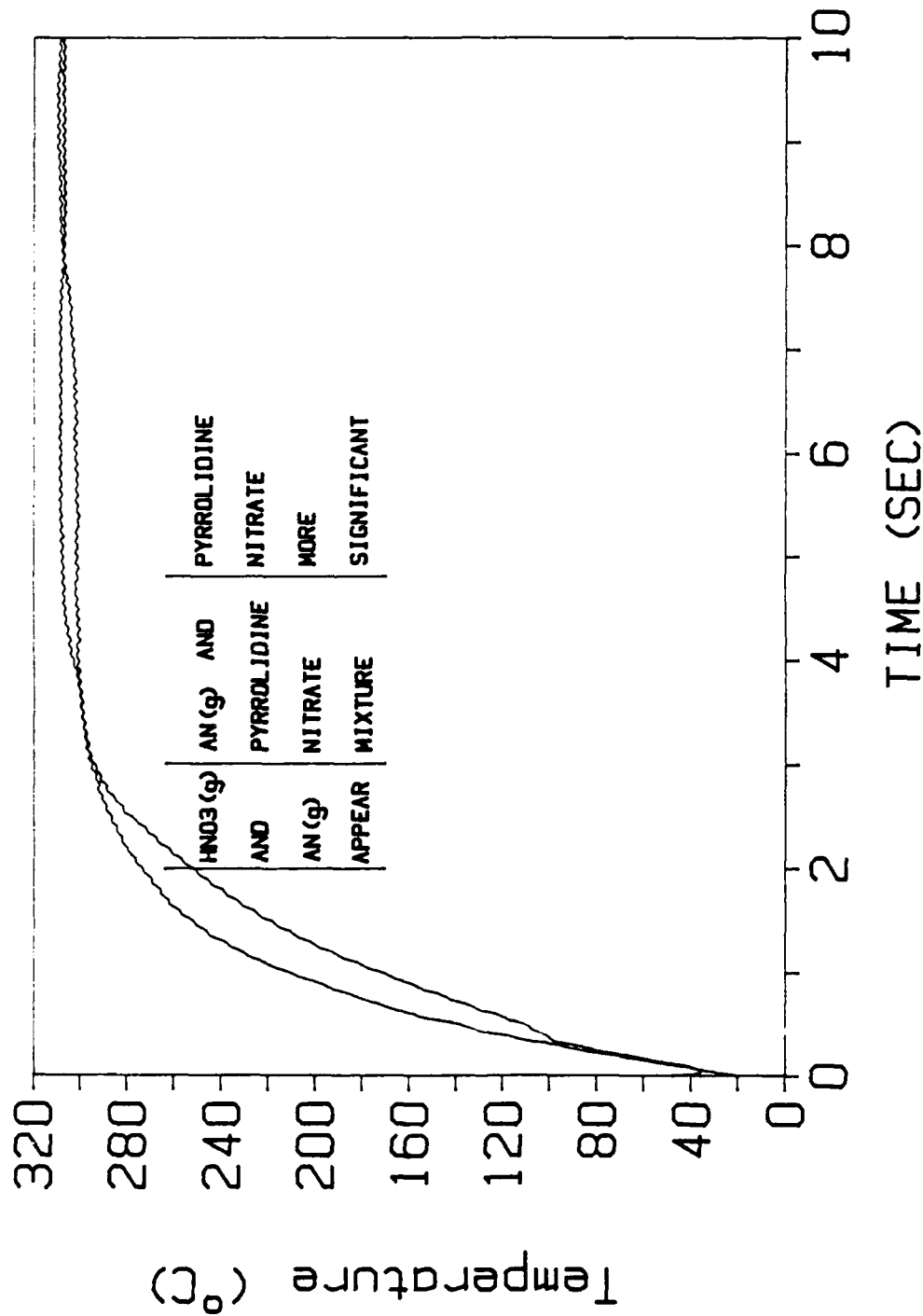
Figure 13.   Thermal Trace of the Condensed Phase BDD Heated at 200°C/sec
to the Decomposition Temperature. The Gas Species Are
Identified in Terms of Their Time of Appearance

31
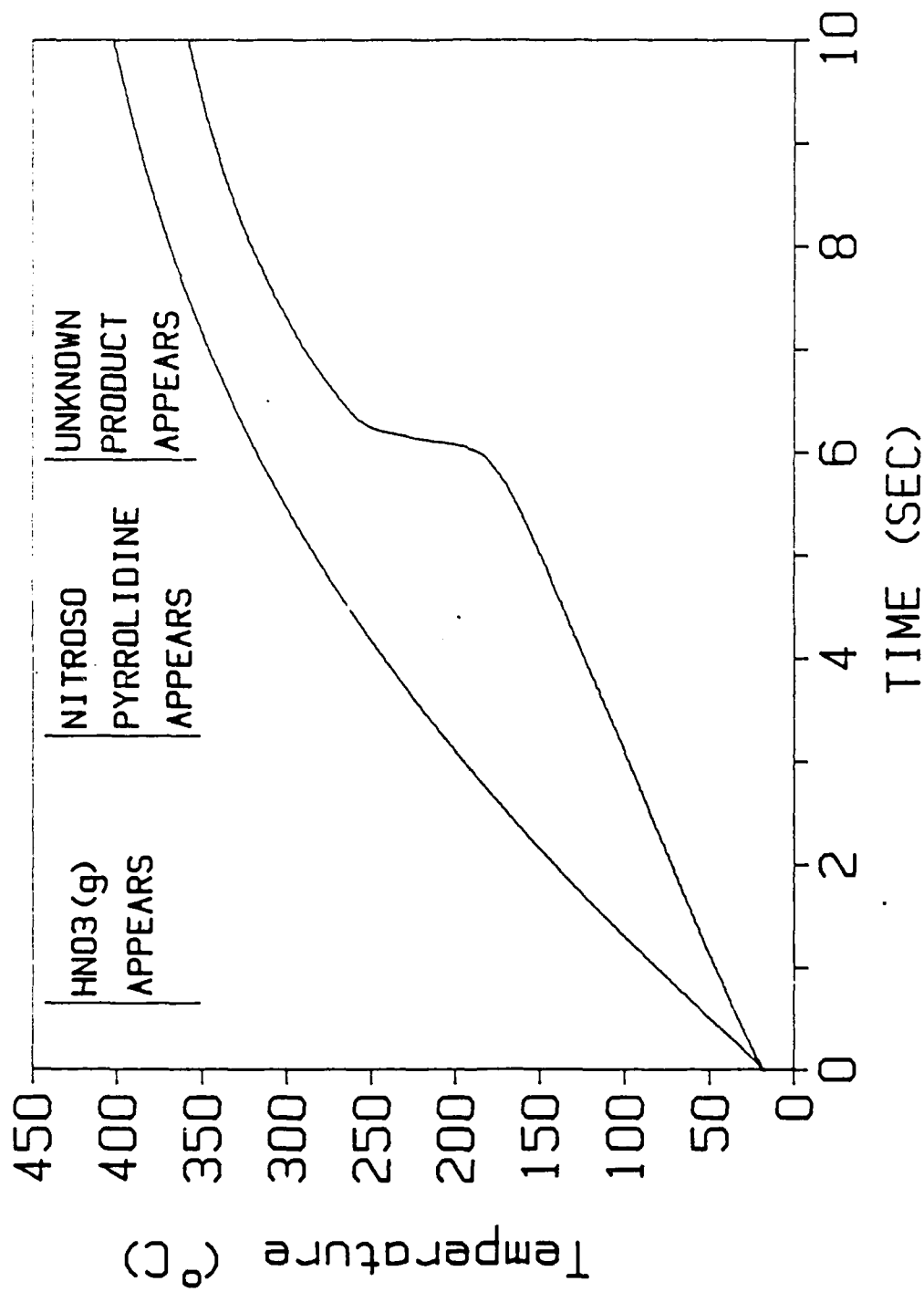
Figure 14. Thermal Trace of Pyrrolidinium Nitrate Heated Through its Decomposition Temperature Range Showing the Products Occurring at Various Times
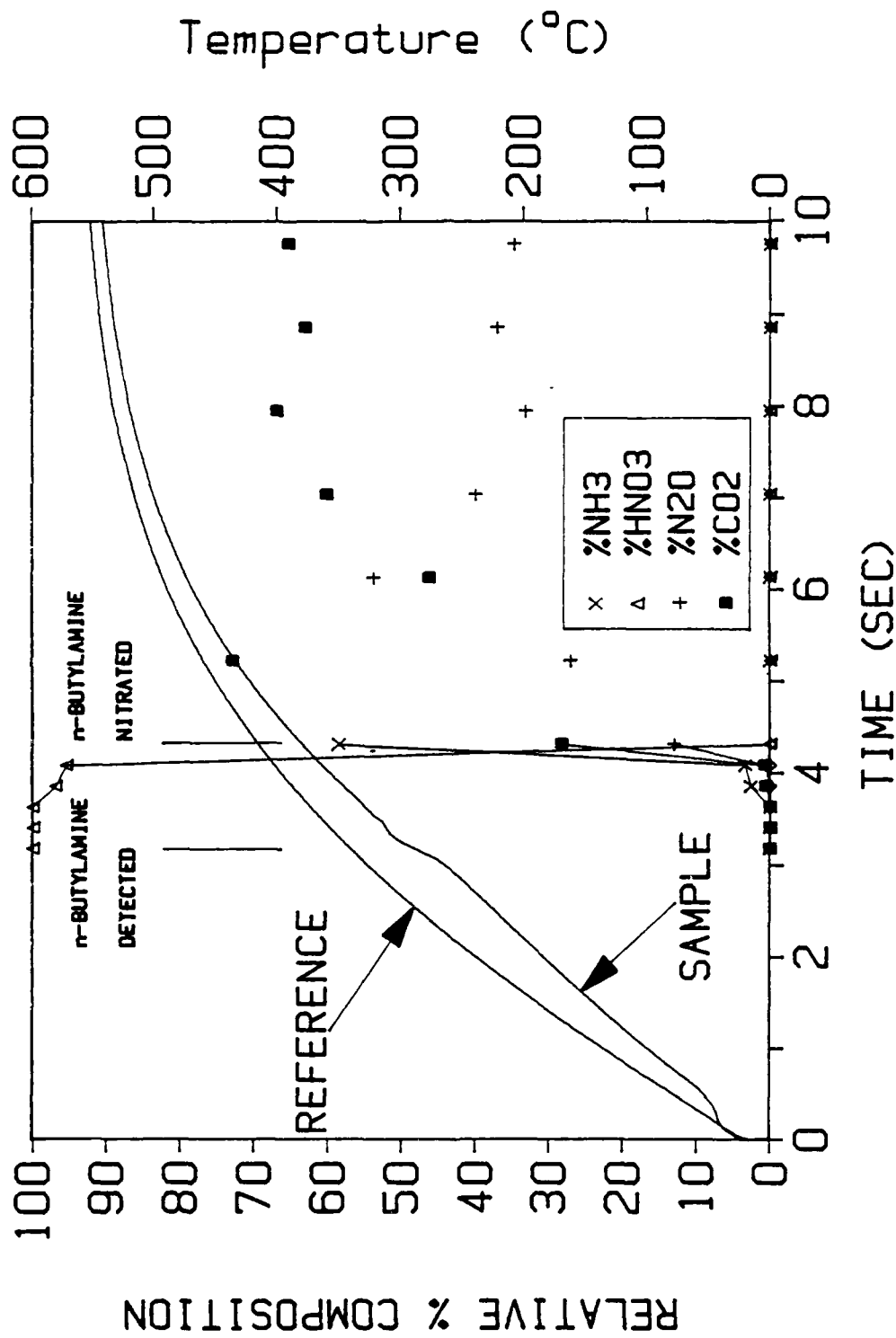
Figure 15. Relative Percent Composition Versus Time Profile for n-Butylammonium Nitrate Under 15 psi Argon When the Sample is Heated at 130°C/sec

33
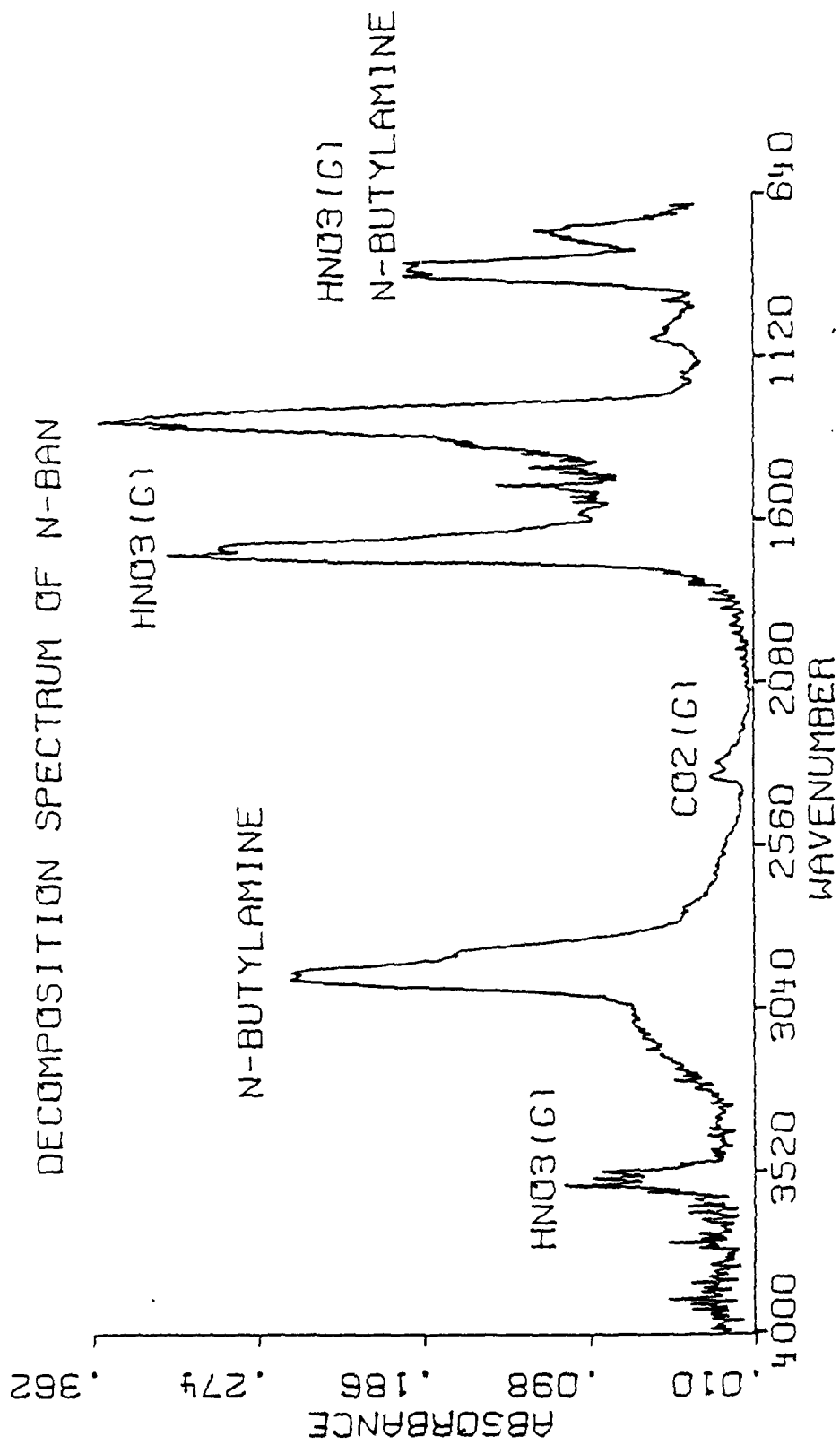
Figure 16. Decomposition Gas Phase Spectrum of n-Butylammonium Nitrate 3.8 sec After the Onset of Heating (from Figure 15)
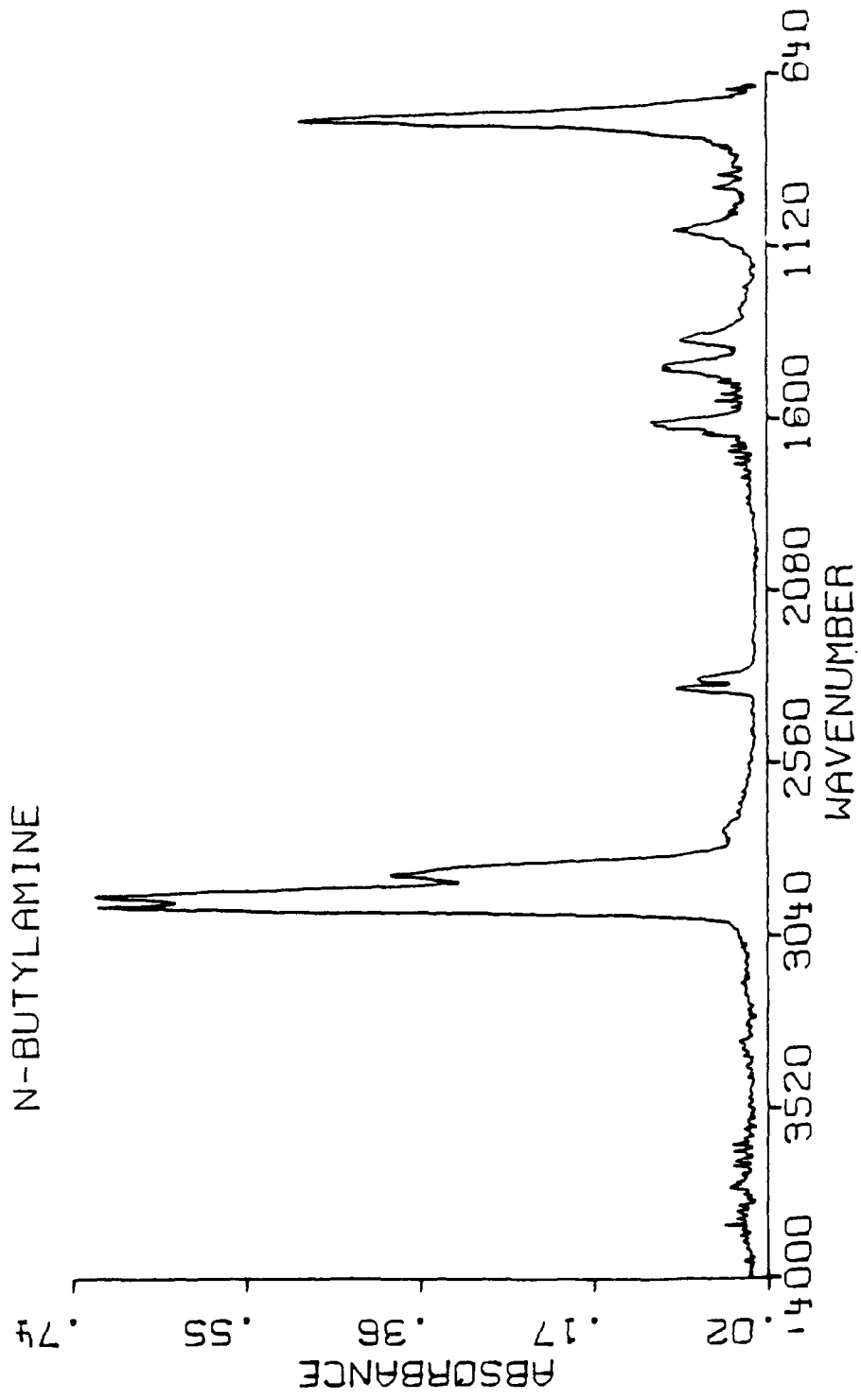
N-BUTYLAMINE

Figure 17.   Gas Phase Spectrum of n-Butylamine

35

DECOMPOSITION SPECTRUM OF N-BAN
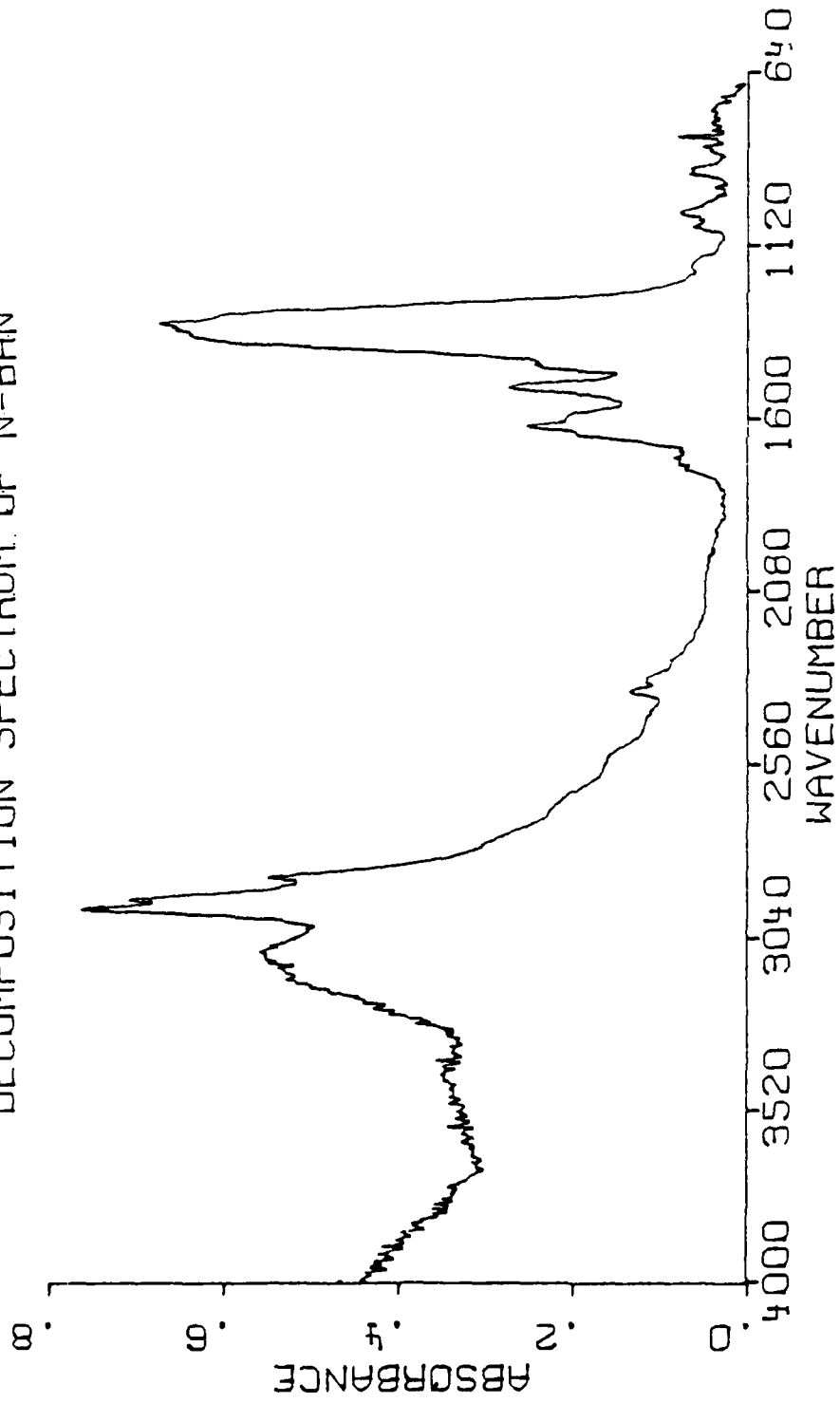
Figure 18.   Decomposition Gas Phase Spectrum of n-Butylammonium Nitrate 4.4 sec After the Onset of Heating (from Figure 15)

N-BUTYLAMMONIUM NITRATE
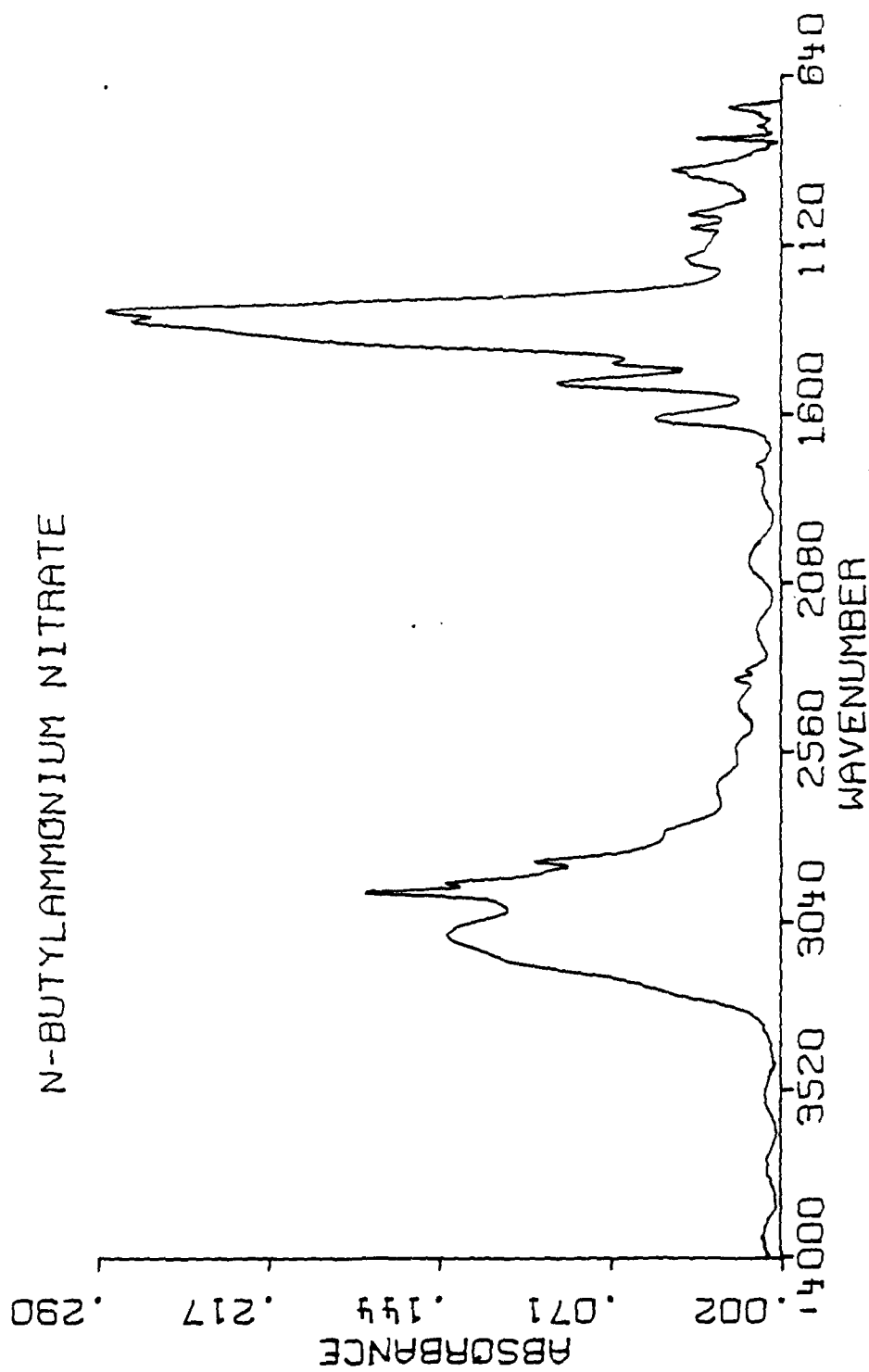
Figure 19.   IR Spectrum of the Solid Phase of n-Butylammonium Nitrate

37
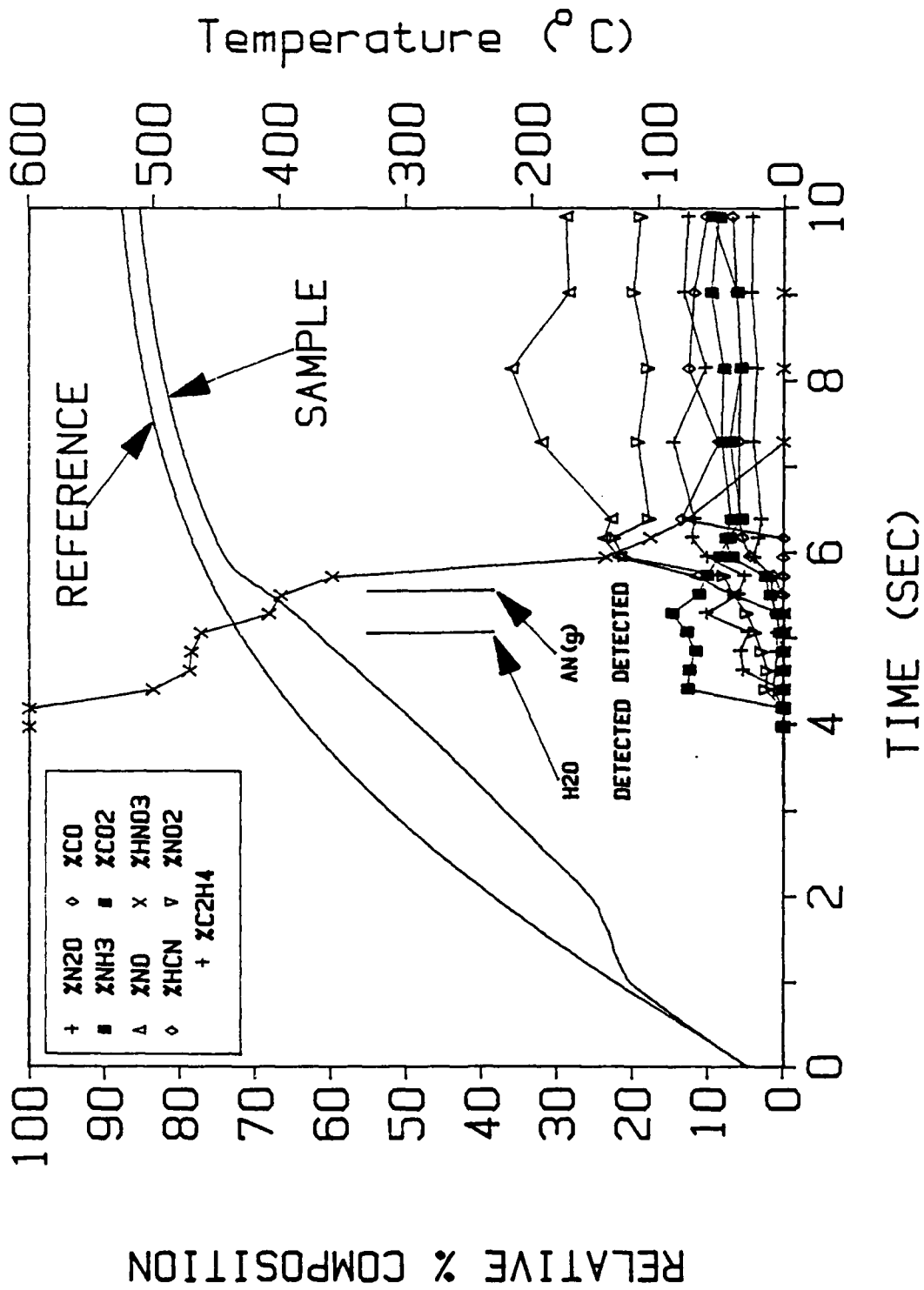
Figure 20. Relative Percent Composition Versus Time Profile for PDD Heated at 140°C/sec Under 15 psi Argon

38
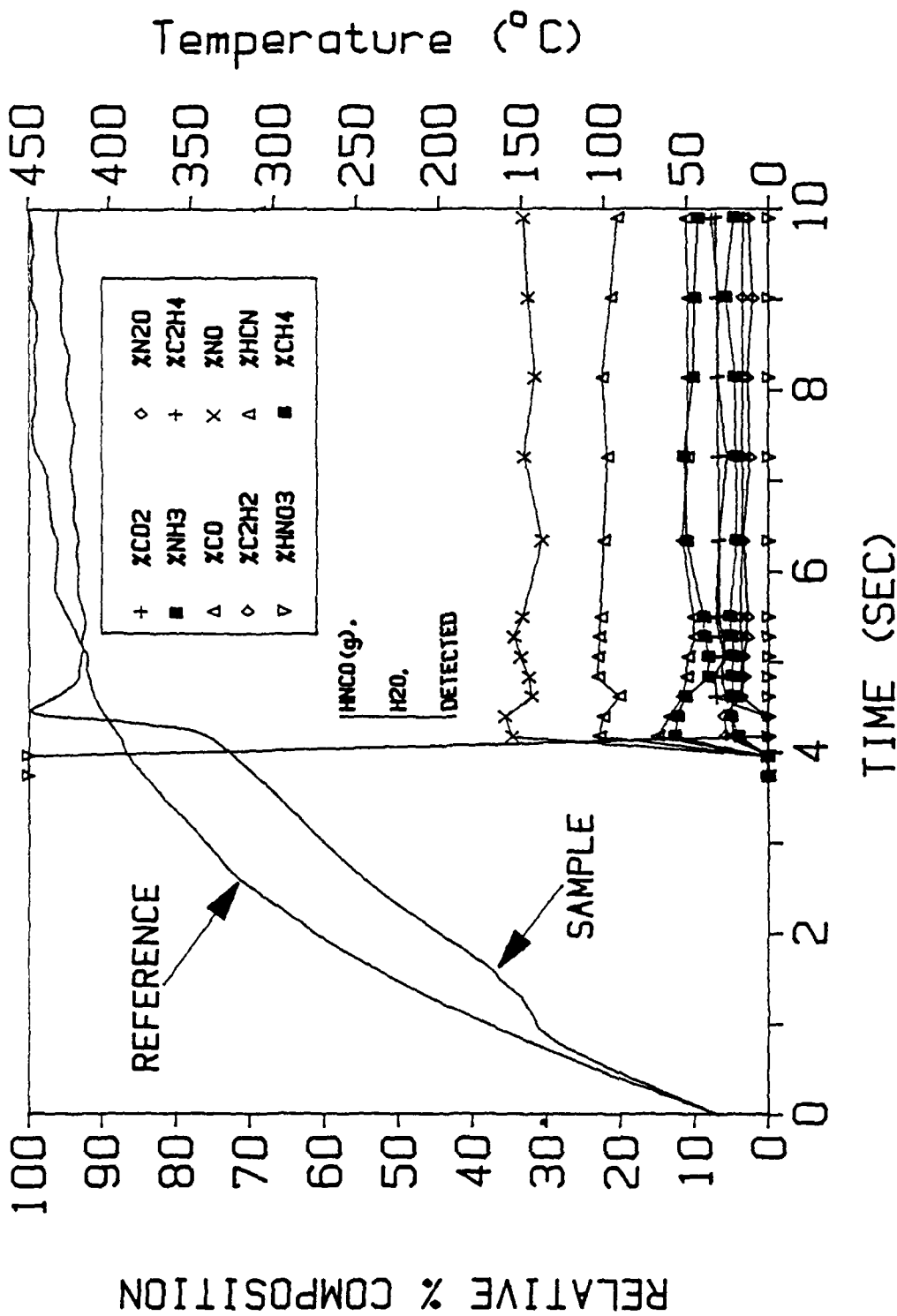
Figure 21. Relative Percent Composition Versus Time Profile for PDD Heated at 140°C/sec Under 200 psi Argon
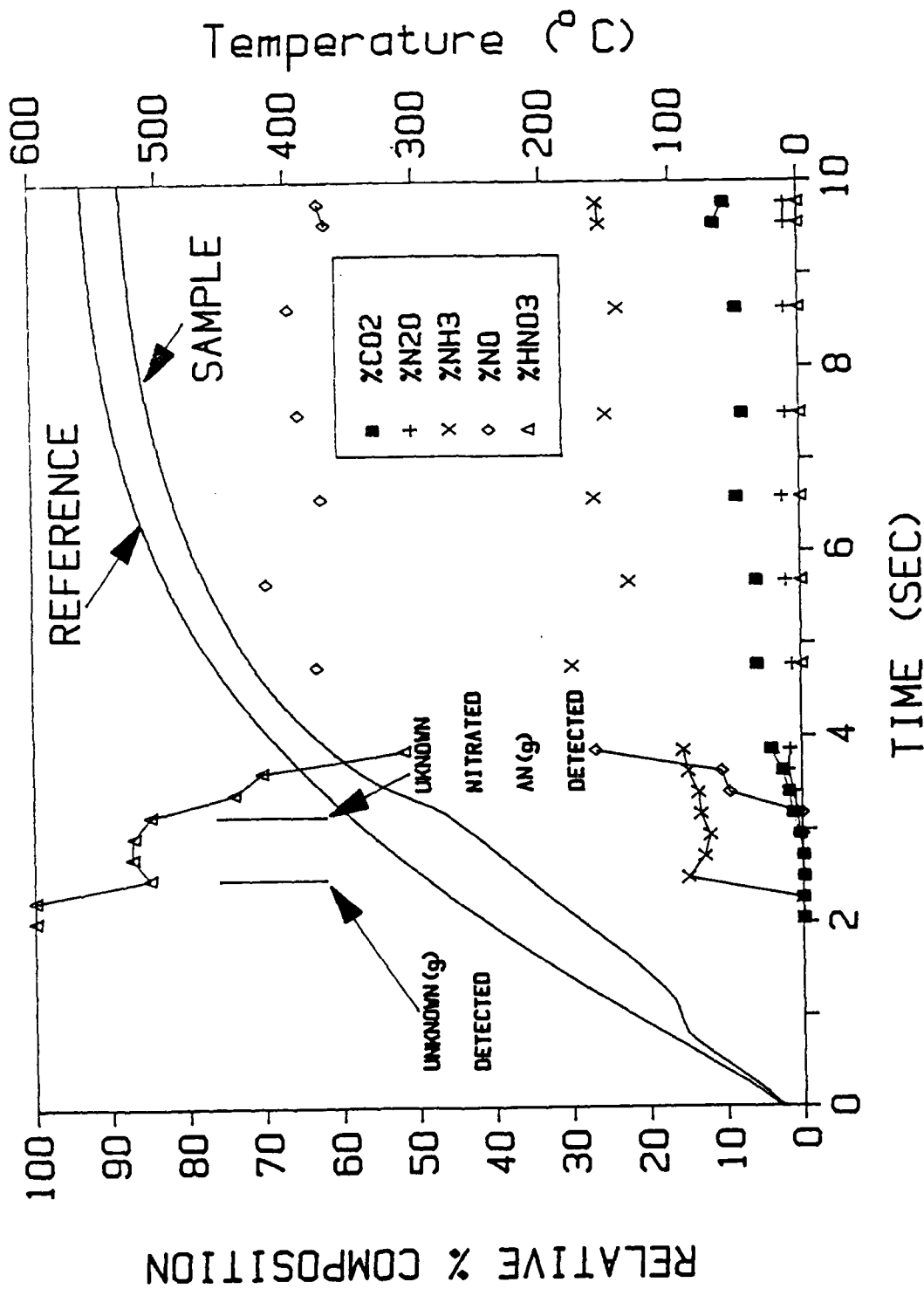
Figure 22. Relative Percent Composition Versus Time Profile for HDD Heated
at 110°C/sec Under 15 psi Argon

40
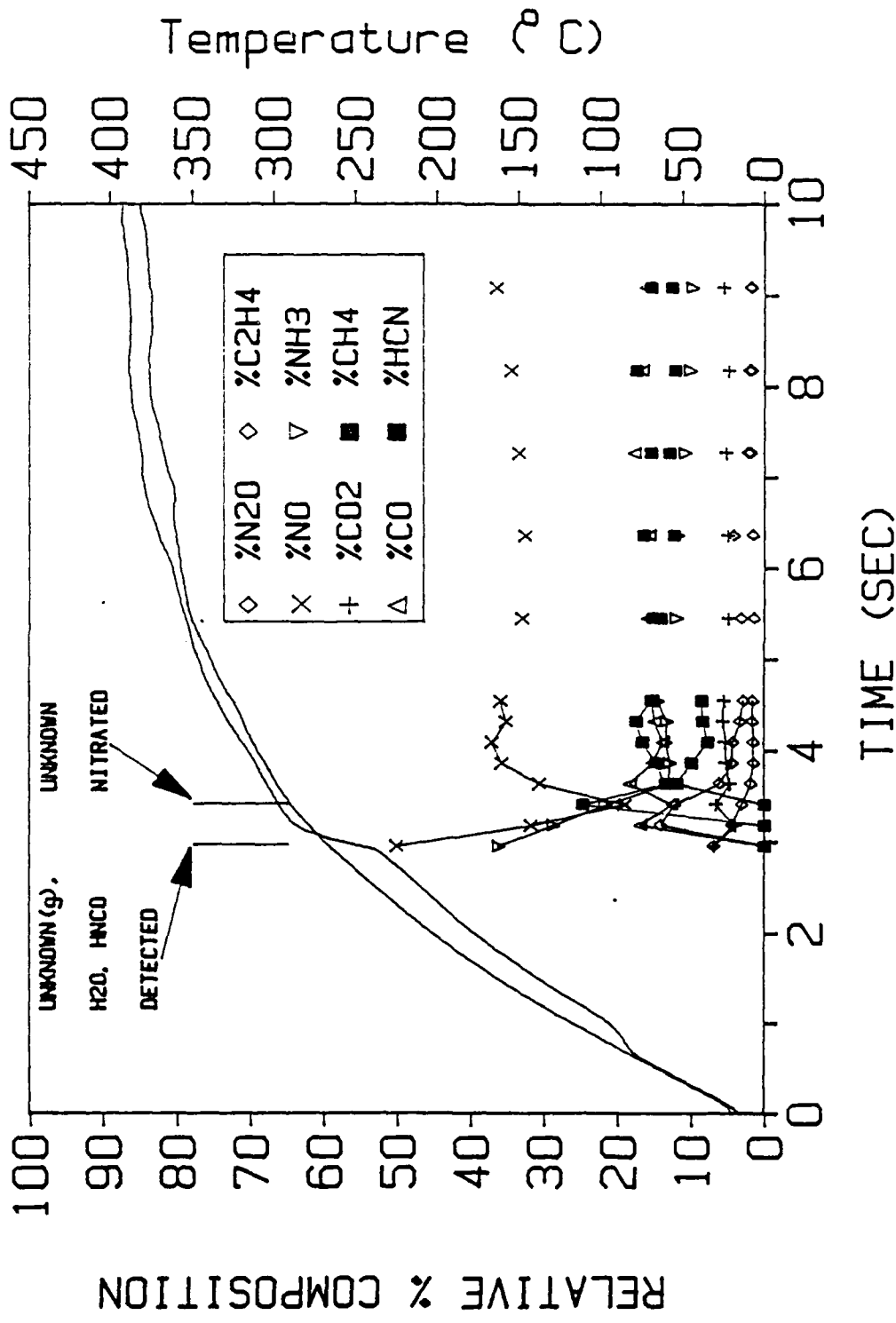
Figure 23. Relative Percent Composition versus Time Profile for IIDD Heated at 110°C/sec Under 100 psi Argon
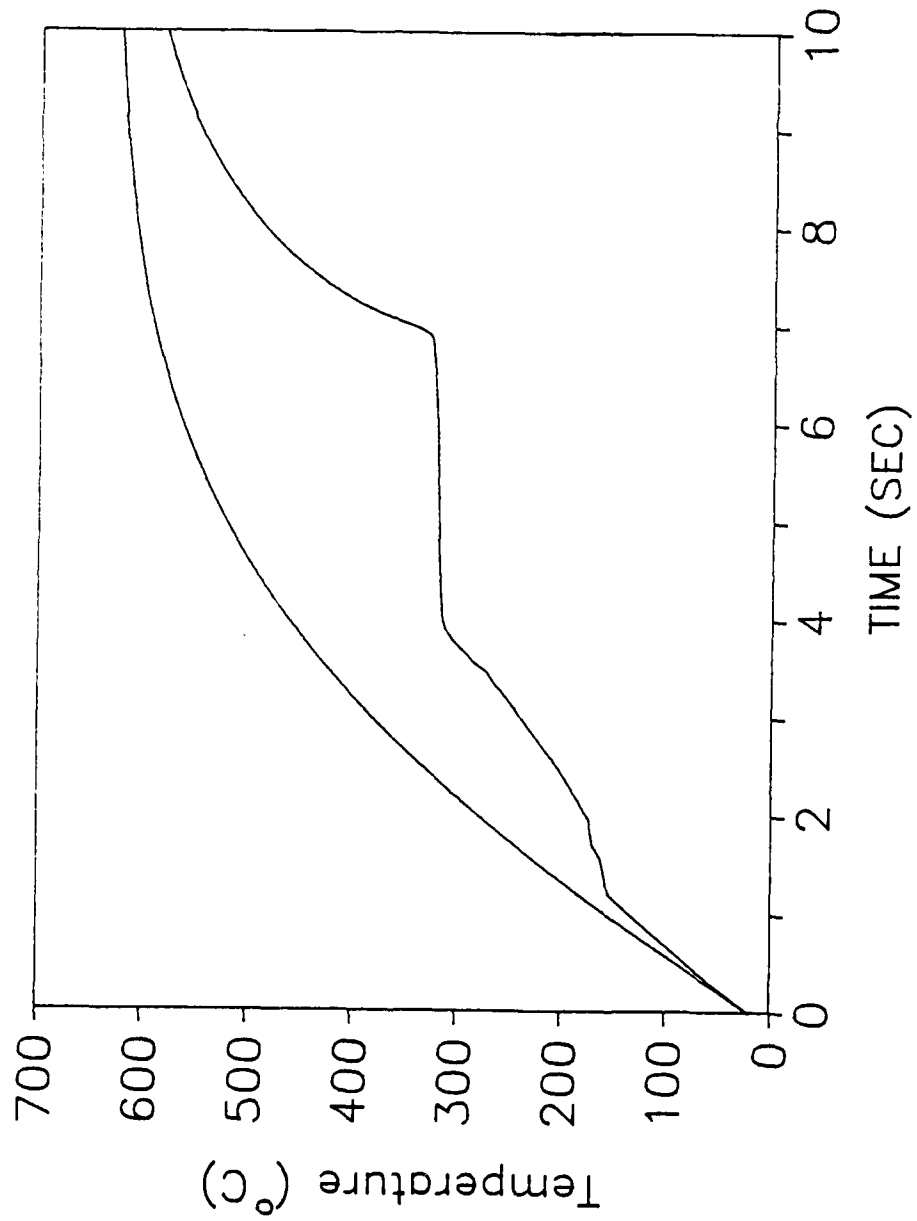
Figure 24.   Thermal Trace of a Sample of Pure Ammonium Nitrate (AN)
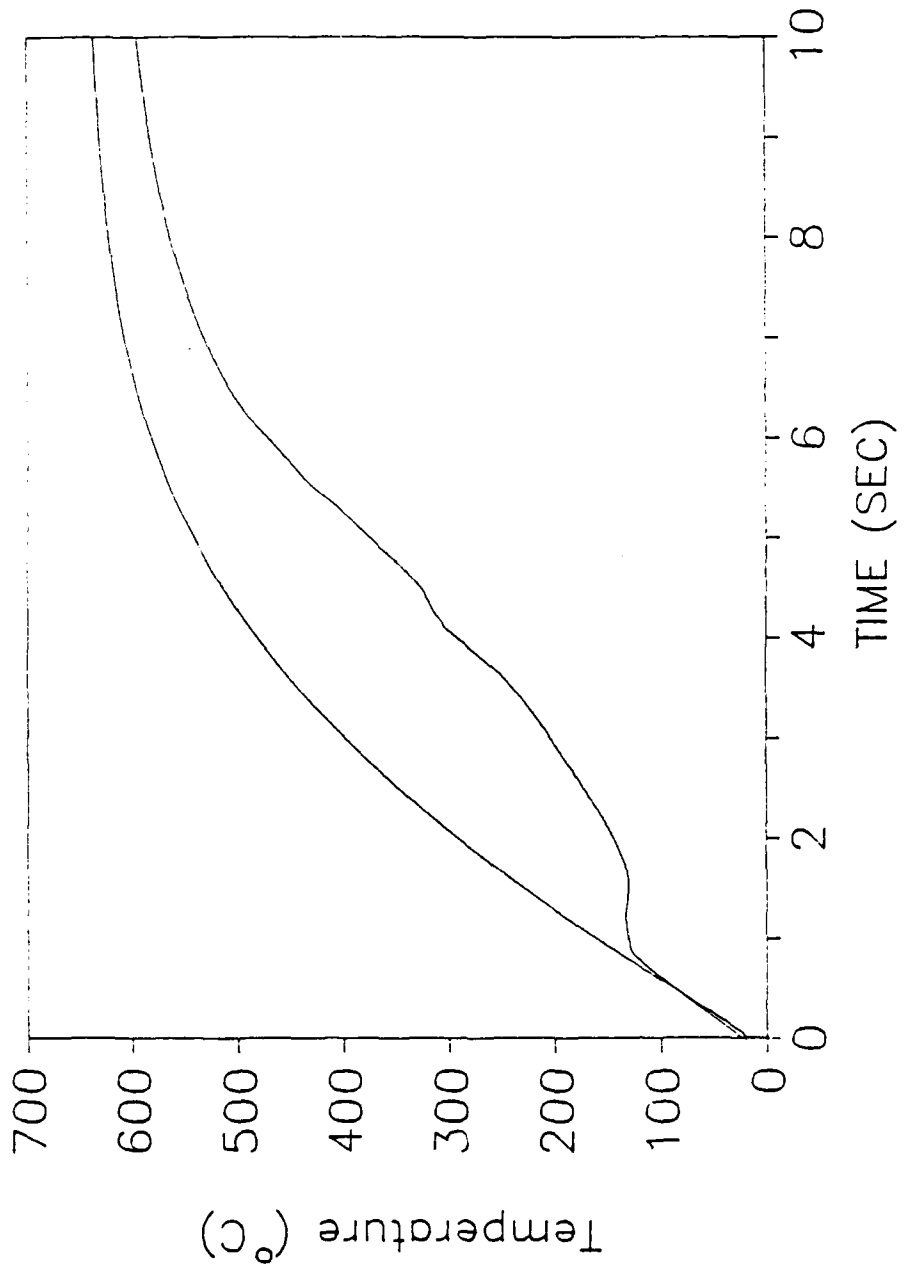
Figure 25.   Thermal Trace of a 25/75 AN/BDO Heterogeneous Mixture

REFERENCES

1. R. J. Karpowicz and T. B. Brill, Applied Spectroscopy, 37, 79 (1983).

2. Y. Oyumi, A. L. Rheingold and T. B. Brill, Propellants, Explosives and Pyrotechnics, 12, 1 (1987).

3. Y. Oyumi, A. L. Rheingold and T. B. Brill, The Journal of Physical Chemistry, 91, 920 (1987).

4. J. T. Cronin and T. B. Brill, Applied Spectroscopy, 41, 1147 (1987).

5. J. T. Cronin, P. Brush and T. B. Brill, to be published.

6. R. L. McKenney, Jr. and S. R. Struck, "Alkylammonium Nitrate Program Review," Florida International University, Miami, FL, Sept., 1987.

7. P. Politzer "Alkylammonium Dinitrate Program Review", Florida International University, Miami, FL, Sept, 1987.

8. Y. Oyumi and T. B. Brill, Combustion and Flame, 68, 209 (1987).